nature protocols

https://doi.org/10.1038/s41596-025-01290-1

Protocol

Check for updates

Visualizing infection by single positive-sense RNA viruses using virus infection real-time imaging (VIRIM)

Lucas J. M. Bruurs[1,4,5], Jelle G. Schipper[2,5], Frank J. M. van Kuppeveld[2] ✉ & Marvin E. Tanenbaum[1,3] ✉

Abstract

To understand viral infection and virus–host interactions, real-time, single-cell assays to track viral infection progression are essential. Many conventional assays sample large numbers of cells for single measurements, averaging out the cell-to-cell heterogeneity that is intrinsic to viral infection. Moreover, conventional assays often require cell fixation or lysis, limiting analysis to a single timepoint and masking the temporal and spatial dynamics of infection. We have developed virus infection real-time imaging (VIRIM), a method to visualize the translation of individual RNAs of viruses in real-time. The single-molecule and live-cell nature of VIRIM allows the examination of the earliest events of viral infection, when viral protein and RNA levels are still low, and allows study into the origins and consequences of cell-to-cell heterogeneity during virus infection. Here we provide a step-by-step description of the VIRIM assay, including a detailed procedure for designing, producing and validating the viruses required for VIRIM. In addition, we provide guidelines for generating the reporter cell line, performing the time-lapse imaging and analyzing the fluorescence microscopy data. Once established, a typical VIRIM experiment requires 2–5 days to complete.

Key points

- Virus infection real-time imaging visualizes viral infection with single viral RNA resolution in live cells using reporter cell lines and time-lapse fluorescence microscopy.
- Virus infection real-time imaging does not require cell fixation or lysis such as many conventional assays, which can limit analysis to single timepoints and mask the temporal and spatial dynamics of infection, and it enables the study of cell-to-cell heterogeneity that is intrinsic to viral infection, unlike many previous techniques.

Key references

Boersma, S. et al. *Cell* **183**, 1930–1945.e23 (2020)

Bruurs, L. J. M. et al. *Nat. Microbiol.* **8**, 2115–2129 (2023)

Schipper, J. G. et al. *PLoS Pathog.* **21**, e1013443 (2025)

[1]Oncode Institute, Hubrecht Institute—KNAW and University Medical Center Utrecht, Utrecht, the Netherlands. [2]Section of Virology, Division of Infectious Diseases and Immunology, Faculty of Veterinary Medicine, Utrecht University, Utrecht, the Netherlands. [3]Department of Bionanoscience, Delft University of Technology, Delft, the Netherlands. [4]Present address: Bilthoven Biologicals B.V., Bilthoven, the Netherlands. [5]These authors contributed equally: Lucas J. M. Bruurs, Jelle G. Schipper. ✉e-mail: F.J.M.vanKuppeveld@uu.nl; M.Tanenbaum@hubrecht.eu

Introduction

Background

The viral life cycle is initiated when a virus particle binds to the host cell and is internalized and the viral genome is released into the host cell cytoplasm. Subsequently, the viral genome undergoes orchestrated cycles of viral genome translation, transcription and replication to generate large numbers of new viral genomes that can subsequently be packaged to form new viral particles[1,2].

Intriguingly, viral infection can progress in a highly heterogeneous manner in different infected cells[2–8]. Such infection heterogeneity could potentially be caused by variability in the expression levels of both pro- and antiviral genes among different cells or as a result of differences in viral genome sequence that are caused by error-prone replication. In addition, stochastic differences in infection, such as the viral entry point in the host cell, the content of the virion or the precise moment or location of viral replication can also impact infection. The earliest stages of infection may be especially important for infection heterogeneity, as small differences in early infection can become amplified during infection to have a major impact on infection outcome. As such, studying early viral infection is important for understanding infection heterogeneity.

Studying these earliest stages of virus infection has remained very challenging because the levels of viral proteins and RNAs are below the detection limit of most assays. Moreover, molecular processes underlying viral infection do not occur synchronously in time. Consequently, classical ensemble measurement assays are not well suited to study these dynamic processes, as they average out highly heterogenous, dynamic and nonsynchronized molecular events. This highlights the need for experimental approaches with single-cell and even single-molecule resolution. Such approaches should have very high sensitivity so that they can detect the low level of viral components during early infection. Moreover, such approaches should preferably be applicable to live cells, as live-cell analysis not only allows the measurements of infection dynamics but also allows the understanding of the consequence of (early) infection heterogeneity. Several high-resolution technologies, including single-cell RNA sequencing (scRNA-seq)[5,6,9–14], single-molecule fluorescence in situ hybridization (smFISH)[15–17] and single virus tracking[18–35] approaches have provided important insight into infection at the single-cell level. However, these approaches either require cell fixation or lysis, or only allow the visualization of viral entry and are limited in providing insights into the dynamics of other early infection processes, such as viral translation and replication. To address this technological gap, we developed virus infection real-time imaging (VIRIM)[2], which allows the visualization of the very first rounds of viral translation and, by extension, replication with single viral RNA resolution by means of live-cell fluorescence microscopy with high spatial and temporal resolution. The highly sensitive, real-time and single-cell nature of VIRIM makes it well suited to elucidate the origins and consequences of cell-to-cell heterogeneity in viral infection.

Different viruses use distinct infection strategies during their life cycle to optimize viral replication, generate viral progeny and escape host cell detection. This is largely dictated by the genetic composition of the virus. We originally developed VIRIM using the positive-sense, single-stranded RNA virus coxsackievirus B3 (CVB3), a representative member of the picornavirus family[36]. Upon entry into the cytoplasm, the CVB3 genome is translated as a single polyprotein that is posttranslationally processed by viral proteases to produce 11 viral proteins, including an RNA-dependent RNA polymerase that replicates the viral genome. With its relatively low genetic complexity and straightforward replication strategy, CVB3 proved to be an ideal system to develop and validate the VIRIM technology. This Protocol will focus on our experiences with picornaviruses, but many aspects of the Protocol will be readily transferrable to other RNA viruses, and we will give generalizable considerations for doing so. Many of the questions relating to cell-to-cell heterogeneity that we studied using CVB3 are equally relevant for other (RNA) viruses. For instance, it has been reported for many viruses that only a small fraction of infections triggers the activation of an interferon-based antiviral response[37]. Furthermore, scRNA-seq and other techniques have revealed a large degree of variation in the

rate of viral infection progression for numerous different viruses[5,6,8–12,14,38–40]. Thus, the VIRIM approach has great potential in studying viral infection dynamics and cell-to-cell heterogeneity in infection for many viruses.

The VIRIM technology

VIRIM is based on a previously developed procedure to visualize the translation of single cellular mRNAs[41–46]. Similar to this technology, termed SunTag translation imaging, VIRIM is comprised of two components: The first component is a viral genomic RNA (vRNA) encoding multiple repeats of the SunTag peptide epitope within the coding sequence of the viral genome (referred to as SunTag-virus). The second component is a single-chain variable fragment antibody that binds to the SunTag epitope and is fused to a fluorescent protein of interest, typically a variant of GFP (referred to as SunTag antibody (STAb)–GFP)[41], which is stably expressed in the host cell. When a SunTag-virus infects a STAb–GFP-expressing cell, the incoming viral genome is rapidly translated by host cell ribosomes. The nascent viral polyprotein contains the array of SunTag epitopes, which are cotranslationally bound by STAb–GFP molecules (Figs. 1 and 2a). vRNAs are typically translated by many ribosomes simultaneously, each of which produces a nascent polyprotein that contains multiple SunTag epitopes, which are bound by STAb–GFP (Fig. 2a). This results in the local enrichment of dozens to hundreds of GFP molecules surrounding actively translating viral genomes[2], which can be readily detected as bright diffraction-limited

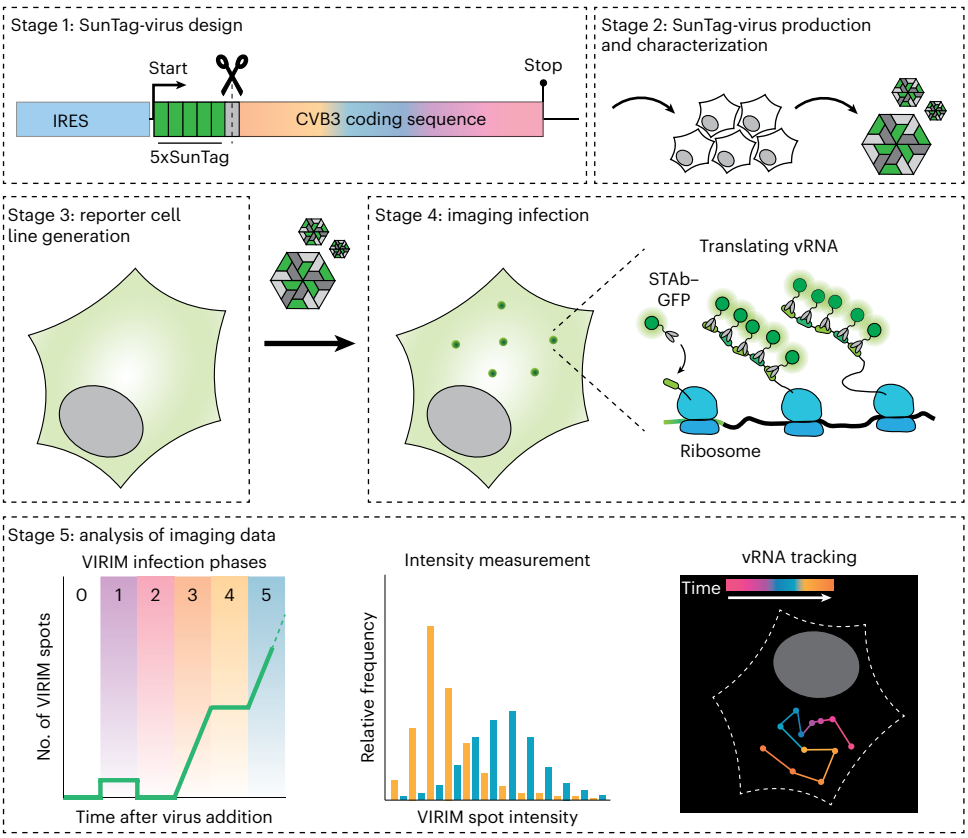

Fig. 1 | Schematic overview of the VIRIM procedure. A typical VIRIM experiment involves several stages: a virus must be engineered that expresses multiple repeats of the SunTag epitope tag (stage 1, Steps 1–5). The SunTag-virus must then be produced and characterized (stage 2, Steps 6–43). In addition to generating a SunTag-virus, a suitable host cell line must be established with stable, low-level expression of the STAb fused to GFP (STAb–GFP) (stage 3, Steps 44–56). In stage 4 (Steps 57–65), the reporter cells infected by the SunTag-virus are imaged by fluorescence microscopy. Finally, the imaging data are processed and analyzed to quantitatively assess various aspects of early virus infection (stage 5, Steps 66–69). In this Protocol, we provide detailed descriptions of three commonly used, different types of analysis: VIRIM infection phase assignment, translation site intensity measurements and measurements of single vRNA mobility through single vRNA tracking.

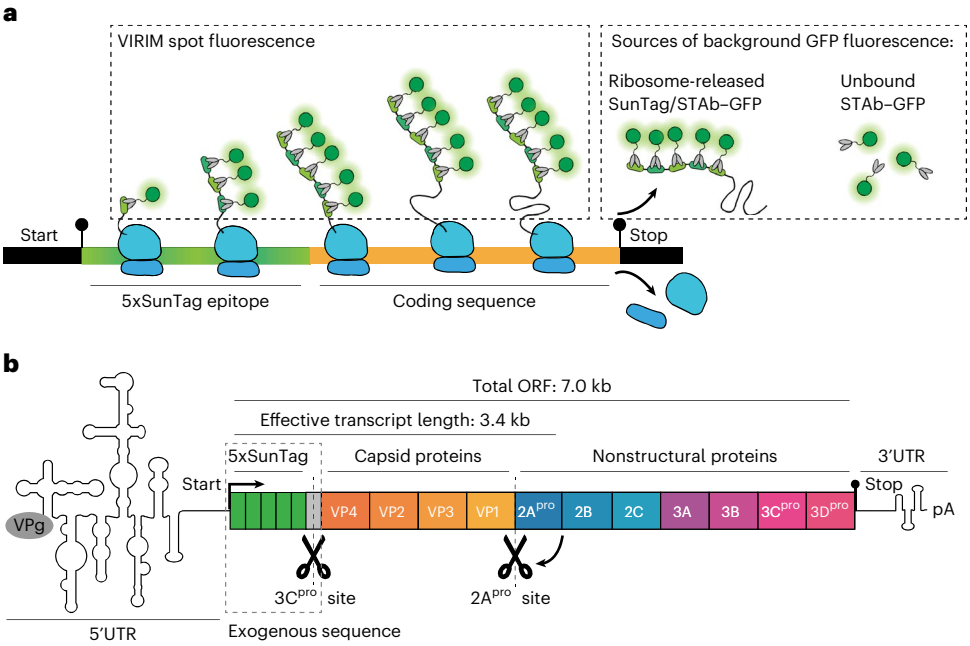

Fig. 2 | VIRIM technology and design of 5xSunTag-CVB3. a, Ribosomes (blue) translating a vRNA that contains a 5xSunTag array (green) and an endogenous coding sequence (orange). Emanating from the individual ribosomes are the nascent chains containing SunTag epitopes, labeled with STAb–GFP. The SunTag/STAb–GFP-containing nascent chains that contribute to VIRIM spot fluorescence are indicated in the left dashed box. The sources of background GFP fluorescence (that is, unbound STAb–GFP and ribosome-released SunTag/STAb–GFP complexes) are indicated in the right dashed box. **b**, The genome architecture of 5xSunTag-CVB3 highlighting important regions of the viral genome and the location of the 5xSunTag array. For SunTag-CVB3, the exogenous sequences that are introduced are composed of the 5xSunTag repeats and the sequence encoding the $3C^{pro}$ cleavage site (indicated by the dashed box). The total length of the coding sequence (7.0 kb) is indicated, as well as the effective length of the transcript encoding the SunTag array (3 kb). The effective transcript length is the vRNA sequence length on which ribosomes are associated with nascent SunTag peptides labeled with STAb–GFP molecules: In the case of CVB3, $2A^{pro}$ is able to cleave the nascent viral polyprotein in *cis* as soon as it is synthesized, thus marking the end of the effective transcript length. This cotranslational processing of the nascent chain results in the release of SunTag/STAb–GFP array from the translating ribosome. Consequently, the ribosomes that are translating the viral ORF downstream of the $2A^{pro}$ sequence are not associated with fluorescent nascent chains and therefore do not contribute to VIRIM foci fluorescence. Viral protein genome-linked (VPg, also known as 3B) is a small virally encoded peptide that is covalently bound to viral rNA and functions as a primer for RNA synthesis during viral RNA-dependent RNA replication. The 5′- and 3′-untranslated regions (UTRs) are viral genome segments before and after the start and stop codons, respectively, and as such are not translated into protein sequences.

fluorescent spots (referred to as VIRIM foci) over the background GFP fluorescence in the cytoplasm.

To reliably detect VIRIM foci, it is important to understand the potential sources of background fluorescence. VIRIM foci formation depends on local enrichment of STAb–GFP molecules at the site of translated vRNAs. The pool of unbound STAb–GFP molecules thus is an important source of background fluorescence. Moreover, once a ribosome completes the translation of the viral genome, the nascent polyprotein that is decorated by STAb–GFP molecules dissociates from the vRNA and diffuses away in the cytoplasm. However, STAb–GFP molecules still bind the ribosome-released SunTag polypeptide (referred to as 'mature' SunTag proteins); therefore, these mature proteins also contribute to the background GFP signal. Importantly, GFP foci corresponding to mature SunTag proteins are typically much dimmer than foci associated with translating vRNAs, as each vRNA is translated by many ribosomes simultaneously, each of which is associated with a fluorescently labeled nascent chain. We found that upon treatment with the translation inhibitor puromycin, all VIRIM foci rapidly disappeared, implying that all observable foci represent actively translating vRNAs, rather than mature SunTag proteins (which are insensitive to translation inhibitors)[2]. Nonetheless, to detect

a VIRIM focus, the STAb–GFP enrichment on a translating vRNA must be strong enough to overcome the baseline GFP fluorescence originating from the unbound STAb–GFP molecules, as well as from STAb–GFP molecules associated with mature SunTag polypeptides.

Importantly, VIRIM only visualizes actively translating vRNAs. For CVB3, we previously demonstrated that the majority of vRNAs in infected cells are being translated at any given time, as determined by VIRIM (~60%). More importantly, the total number of vRNAs, as determined by smFISH, correlates very well with the number of VIRIM foci throughout early infection ($R^2 = 0.90$) (ref. 2). Consequently, the number of VIRIM foci can be used to assess the number of vRNAs per cell and thus to determine viral replication rates over time. Moreover, picornavirus vRNAs undergo translation rapidly upon entry into the host cell cytoplasm; therefore, VIRIM also allows the accurate determination of the moment of viral entry. Finally, translation and replication use the same vRNA template but occur with opposite directionality (5′ to 3′ and 3′ to 5′, respectively). Therefore, these processes cannot occur at the same time on a single vRNA. As such, translation initiation must shut down, and all ribosomes that have already initiated translation must complete translation before replication can initiate[47,48]. As the shutdown of translation results in the disappearance of VIRIM foci, the VIRIM assay indirectly reports on replication[2]. Together, VIRIM has broad applications in studying viral infection.

Applications of VIRIM

SunTag translation imaging of mRNAs has been extensively used to assess various aspects of mRNA biology, including translation dynamics and efficiency[44] but also translation quality control[49] and localized translation[50]. VIRIM enables the same types of analysis for viral translation. In addition, because the number of VIRIM foci can be used as a proxy for the total number of vRNAs in the cell, VIRIM also provides information about the moment of viral entry and replication, as well as viral replication rates. In our initial work on CVB3, this allowed us to discriminate different phases during early infection that are indicative of alternating rounds of vRNA translation and replication. The evaluation of these infection phases not only provided insights into the duration of different steps of viral infection, which was highly divergent among infections, but also identified bottlenecks for successful infection. For instance, we found that a considerable fraction of CVB3 infections have successful initial translation but fail during initial replication, identifying the replication of the incoming vRNA as an important bottleneck for infection progression.

VIRIM can also be used to study the dynamics of virus–host interactions. During CVB3 infection, the viral 2A protease rapidly cleaves eukaryotic translation initiation factor 4G (eIF4G) and the integral nuclear pore component nucleoporin 98 (NUP98), resulting in a selective shutdown of host translation and the disruption of nucleocytoplasmic trafficking, respectively[51–58]. By combining VIRIM with reporters of host translation or nuclear pore integrity, we could demonstrate that CVB3 infection results in compromised nuclear pore integrity and inhibition of host translation even before the first round of viral replication, emphasizing the potency of viral proteases in altering the host cell environment[2]. Furthermore, when combining VIRIM with a readout for innate immune activation, we could link variation in early viral replication rates with differences in antiviral response activation later in infection[1]. Finally, we recently used VIRIM to illuminate the role of the viral 2A protease during early CVB3 infection[59].

Aside from studying (heterogeneity in) viral translation and replication dynamics, and its effects on infection progression and the host cell, VIRIM also allows the effect of host factors and antiviral signaling on virus infection dynamics to be examined. For example, we were able to perform a small-scale screen to identify specific interferon-stimulated antiviral genes that restrict CVB3 infection during the initial cycle of vRNA replication[2].

VIRIM can also be combined with other labeling strategies. For example, the direct visualization of viral RNA could be achieved by employing RNA aptamers[60–62] or the MS2–PP7–RNA labeling system[63–65]. Moreover, other viral proteins or host factors could simultaneously be tagged with other (split) fluorescent proteins. For example, we previously successfully tagged the CVB3 3A protein, which localizes to viral replication organelles, with GFP-S11 (ref. 66). Combining the fluorescent 3A protein with VIRIM would enable the examination of the connection between viral translation and replication organelle formation.

Comparison of VIRIM with other techniques

Many powerful techniques are available for studying viral infection with single-cell resolution. Each technique has its own advantages and limitations, and no single technique can substitute for all other approaches. VIRIM expands the toolbox of the virologist by offering a real-time readout of virus infection with single-molecule sensitivity.

Infection in single cells can be visualized by antibody-based staining of viral and host proteins. Immunofluorescence is relatively simple and has been broadly applied to many viruses. Immunofluorescence allows the visualization of viral protein levels and localization in single cells and thus provides a robust readout of viral infection progression. Drawbacks of immunofluorescence are that the assay requires unique antibodies for each virus, which are not readily available for poorly studied viruses and are expensive and time-consuming to produce. In addition, immunofluorescence is not sensitive enough to detect single viral molecules and is thus not ideally suited to study the very early stages of infection. Finally, immunofluorescence requires cell fixation and permeabilization for antibody penetration into cells. Therefore, immunofluorescence fails to report on temporal dynamics, which is critical to fully understand dynamic processes such as viral translation and replication. Moreover, the lack of temporal information makes it difficult to establish direct causal relationships between events occurring at distinct times during infection, for example, how early infection heterogeneity impacts infection outcome.

Similar to immunofluorescence, fluorescence-activated cell sorting (FACS) enables antibody-based measurements of viral and host protein levels in single, fixed cells. FACS facilitates a high-throughput measurement of many single cells, providing an advantage over immunofluorescence. However, FACS does not provide information on protein localization within cells.

smFISH enables the visualization of single viral RNAs via hybridization with complementary fluorescent DNA probes. Similar to VIRIM, smFISH achieves single-molecule resolution and has been used to study the earliest phases of viral infection[15–17]. Whereas VIRIM only visualizes translated vRNAs, smFISH labels all vRNAs in a cell. Furthermore, the viral negative strand replicative intermediate, which marks the sites of replication, can also be detected by smFISH using an adapted protocol[16]. The genetic manipulation of the virus (or host cell) is not required for smFISH, and it is thus easily adaptable to divergent experimental needs. An additional benefit of smFISH is that it also allows expression levels of multiple mRNAs per cell to be assessed, enabling the simultaneous measurements of different viral RNAs or both viral and host RNAs. Measuring both viral and host RNAs can prove especially powerful when combined with live cell readouts for viral infection dynamics, for example, to yield insights on the dynamic interplay between virus and host[1].

Similar to smFISH, scRNA-seq provides information on viral and host mRNA levels in cells[5,6,9–14]. The advantages of scRNA-seq over smFISH are that the levels of all viral and host RNAs can be measured in each cell simultaneously. However, scRNA-seq has a lower sensitivity than smFISH and is therefore less well suited for studying early infection. Moreover, scRNA-seq does not provide information on RNA localization in infected cells.

In addition to fixed-cell approaches, several live-cell assays for studying virus infection have previously been developed. Most notably, (split) GFP-encoding viruses have been broadly applied to study infection progression for many viruses[1,8,66–72]. The major advantage of GFP-encoding viruses is that they provide a simple, quantitative readout of viral infection progression. However, compared with GFP viruses, VIRIM offers superior detection sensitivity, as virus-encoded GFP typically requires multiple hours for the buildup of GFP protein levels to reach the detection threshold. By contrast, VIRIM can visualize the translation of the very first incoming vRNA. In addition, VIRIM allows the independent assessment of both vRNA translation and replication, whereas GFP viruses only report on viral protein levels, which is dependent on both viral translation and replication. Inversely, GFP viruses are more suitable for studying later infection, as the VIRIM assay predominantly captures the early phases of infection (‘Limitations’ section).

Several live-cell single-molecule imaging approaches for the visualization of viral entry and genome release into the host cell have also been developed previously. These strategies involve

the fluorescent labeling of viral particles; either the capsid, membrane or vRNA[18–31]. The main advantage of these approaches compared with VIRIM is that visualization does not require vRNA translation; therefore, the viral entry can be studied with a higher temporal precision. Moreover, the incoming viral particle constitutes the sole source of fluorescent signal in the image, resulting in high signal-to-noise images. The downside of approaches that label the incoming particle is that they allow only the visualization of the process of cell entry but do not label the vRNA translation or replication. Such particle labeling strategies can, in principle, also be combined with VIRIM, providing a detailed view of both viral entry and postentry processes for the same infection.

Limitations

Although VIRIM offers various advantages compared with other techniques to visualize (early) virus infection, it also has several important limitations, which are outlined below.

First, VIRIM requires the genetic modification of both the virus and the host cell to visualize the viral infection. Introducing the repeats of the SunTag epitopes in the viral genome can be particularly challenging, as large exogenous sequences may not be stably maintained in the viral genome during viral passages, and such insertions could impact viral fitness. Finding an appropriate insertion site for the SunTag array in the viral genome may require several rounds of trial and error. In this Protocol, we provide detailed considerations for design of the SunTag-virus.

Second, because of the requirement for genetic engineering of the virus and host cell, VIRIM can only be applied to viruses for which a (reverse) genetics system is available and in cell types that can be engineered to stably express the STAb–GFP. As such, it is more challenging to adapt VIRIM to clinical isolates of a virus or to primary cells that cannot be efficiently engineered.

Third, VIRIM only visualizes translating vRNAs, meaning that the fraction of translationally inactive (for example, replicating, defective or putatively dormant vRNAs) cannot be directly observed. Replication can, however, be inferred from the increase in the number translation sites. Moreover, combining VIRIM with smFISH labeling of both positive and negative strands for the same cells can give insights into translation, while also directly visualizing translationally silent vRNAs.

Finally, VIRIM is not well suited to study the later stages of infection. First, it relies on visualization and counting of individual foci, and once their number increases to hundreds or more, individual foci can no longer be easily distinguished. In addition, as infection progresses, there is a continuous increase in the number of mature, ribosome-released SunTag polypeptides, which also bind to STAb–GFP molecules. As such, these mature peptides will ultimately sequester all the available STAb–GFP in a cell, resulting in a decreased labeling efficiency of nascent SunTag peptides emanating from actively translated vRNAs (in a process referred to as 'antibody depletion'). After substantial antibody depletion, individual translating vRNAs can no longer be observed. For CVB3 in our STAb–GFP cells, antibody depletion typically occurs 4–6 h after the translation of the incoming vRNA initiates, although the precise moment of antibody depletion is probably different for other viruses and cell lines. Even though antibody depletion typically caps the total time that viral infection can be tracked using VIRIM, VIRIM still facilitates the correlation of events in late infection (for example, antiviral response activation) to the dynamics of early infection.

Experimental design

A typical VIRIM experiment involves the design and production of the SunTag-virus (stages 1 and 2), the generation of a STAb–GFP expressing reporter cell line (stage 3), imaging the infection and analyzing the data (stages 4 and 5; Fig. 1). In this section, we provide guidelines for the experimental design for each stage of a VIRIM experiment.

Stage 1: SunTag-virus design

SunTag integration site: finding the optimal site for the introduction of the SunTag peptide array in the viral genome is possibly the most critical aspect of the VIRIM methodology. Viruses have evolved extremely efficient usage of their genetic capacity, and the introduction

of exogenous sequences frequently affects viral fitness. The ability of a virus to tolerate insertions will vary between viruses and on the exact site of the SunTag integration. It is often difficult to predict whether a specific site tolerates the SunTag insertion, and exploring several different designs will probably be worth the initial investment. In the case of picornaviruses, we introduced the SunTag array at the extreme N-terminal side of the viral polyprotein (Fig. 2b).

To identify candidate sites for SunTag insertion in the viral genome, the following general strategy can used:

- Identify sites in the viral genome that have been successfully used before to introduce exogenous sequences, such as GFP. These sites are likely to also tolerate the insertion of the sequence encoding the SunTag epitopes. The introduction of the SunTag array at a site in the viral genome that has not been used before to engineer the virus may be pursued, but in this case, targeting multiple sites may be needed to identify a site that is tolerated by the virus
- Identify sites in a long open reading frame (ORF): longer ORFs are typically translated by more ribosomes simultaneously, thus resulting in the production of more SunTag nascent polypeptides that are simultaneously associated with a vRNA, which in turn results in the recruitment of more STAb–GFP molecules, providing a brighter VIRIM spot (Fig. 3). Of note, many viral ORFs encode a large polyprotein, which, upon translation, is separated to yield individual proteins. The polyprotein processing generally occurs either via cotranslational proteolytic processing by virally encoded proteases or by the inclusion of so-called ribosomal skipping sequences (for example, the self-cleaving 'T2A' sequence), which cause a failure in peptide bond formation by the ribosome between adjacent viral proteins. Polyprotein cleavage or failures in peptide bond formation result in the release of the upstream SunTag sequence with its associated STAb–GFP molecules, which will diffuse away from the vRNA, reducing the overall VIRIM signal. Therefore, the presence of such sequences or the relative location in the ORF of proteases responsible for polyprotein separation should be considered when designing the SunTag-virus to ensure that SunTag-STAb–GFP complexes remain associated with the vRNA as long as possible
- Preferably position the SunTag repeats at the 5′ end of a viral ORF. By positioning the SunTag peptide epitopes at the N-terminus of a viral protein, a larger fraction of the ribosomes associated with the vRNA will be associated with nascent SunTag peptides, generating a brighter VIRIM signal (Fig. 3)

Number of SunTag peptides: once the candidate integration sites for the SunTag epitopes have been identified, it is important to consider the number of SunTag repeats that are introduced at these sites. Although more SunTag repeats will result in stronger STAb–GFP accumulation at translating vRNAs and therefore brighter VIRIM foci, there typically is a limit to the size of the exogenous sequences that can be stably introduced in a viral genome without compromising viral fitness. The number of repeats that is required for single vRNA detection strongly depends on the insertion site (that is, on the ORF length and position within the ORF; Fig. 3) and, additionally, on the translation initiation rate of the vRNA, where a higher translation initiation rate results in a higher ribosomal load on vRNAs and thus more fluorescence signal per vRNA. Five repeats of the SunTag epitope, linked by short glycine–serine spacer sequences (GSGSG), are encoded by ~350 nt, which is shorter than, for instance, the sequence encoding GFP (~700 bp). However, depending on the ribosome initiation rate and the downstream ORF length, 12 or 24 copies of the SunTag epitope may be required to obtain the sufficient VIRIM signal. To observe a GFP focus on a spinning disk confocal microscope, ~10–40 GFP molecules are typically needed in a single diffraction-limited spot, depending on the background fluorescence of the cells, the brightness of the fluorescent protein and the sensitivity of the camera. For our studies on picornaviruses, we made use of five copies of SunTag, and these were followed by a 3.0–3.1 kb ORF sequence, which results in foci that are easily detected on our microscope (spinning disk confocal microscope with a sensitive scientific complementary metal–oxide–semiconductor (sCMOS) camera; Fig. 2b).

SunTag fusion with viral proteins: it is also important to consider whether the SunTag array will interfere with the function of the viral protein to which it is fused. Although the SunTag epitopes are important in the nascent chains for the visualization by VIRIM, the fusion

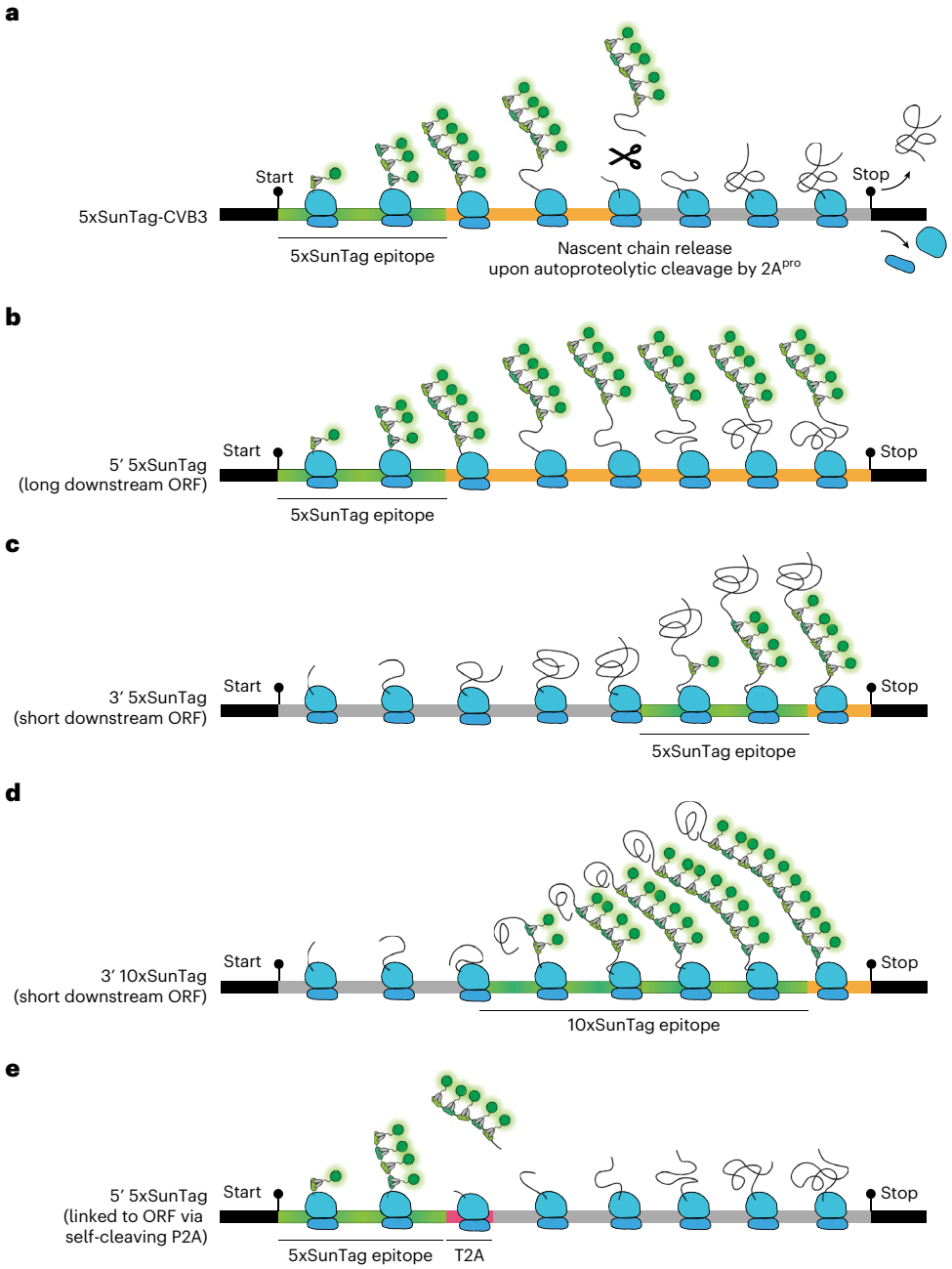

Fig. 3 | Design principles for generating SunTag-virus. A schematic representation of vRNAs with SunTag peptides inserted in different positions of the genome. These examples illustrate how the SunTag position and length, as well as the downstream ORF length, affect the number of STAb–GFP molecules on the translating vRNA (and consequently, VIRIM spot intensity). **a**, An illustration of the 5xSunTag-CVB3 virus in which the 5xSunTag array is inserted at the 5′ end of the viral ORF. The black scissors indicate the cleavage event that results in nascent chain release from the translating vRNA and concomitant dissociation of STAb–GFP molecules from the translating vRNA. **b**, The 5xSunTag array positioned at the 5′ end of a long ORF on which fluorescently labeled nascent chains remain associated with the translating vRNA until the stop codon. Because the SunTag-containing nascent chains remain associated with the translating vRNA for a longer time, the VIRIM spots will be brighter in this situation compared with the 5xSunTag-CVB3 shown in **a**. **c**, The 5xSunTag array positioned more towards the 3′ end of the ORF. Because the ORF downstream of the SunTag array is substantially shorter in this situation, fewer SunTag-containing nascent chains are associated with the translating vRNA compared with a vRNA in which the SunTag array is positioned at the 5′ end **b**. **d**, Introducing a 10xSunTag array results in brighter VIRIM foci compared with **c** because the SunTag coding sequence is longer, allowing the accumulation of more fluorescently labeled nascent chains, and because a single nascent chain can be labeled by more STAb–GFP molecules (maximum ten instead of five). **e**, The introduction of a self-cleaving T2A sequence downstream of the 5xSunTag array, for instance, to prevent the potential interference of the SunTag array with viral protein function, reduces the VIRIM spot intensity because of premature nascent chain release. In all schematics, translating ribosomes are depicted in blue. The SunTag coding sequence is indicated in green, viral ORFs that contribute to VIRIM spot intensity are indicated in orange and the part of the viral ORF that is not contributing to VIRIM spot intensity is colored in gray.

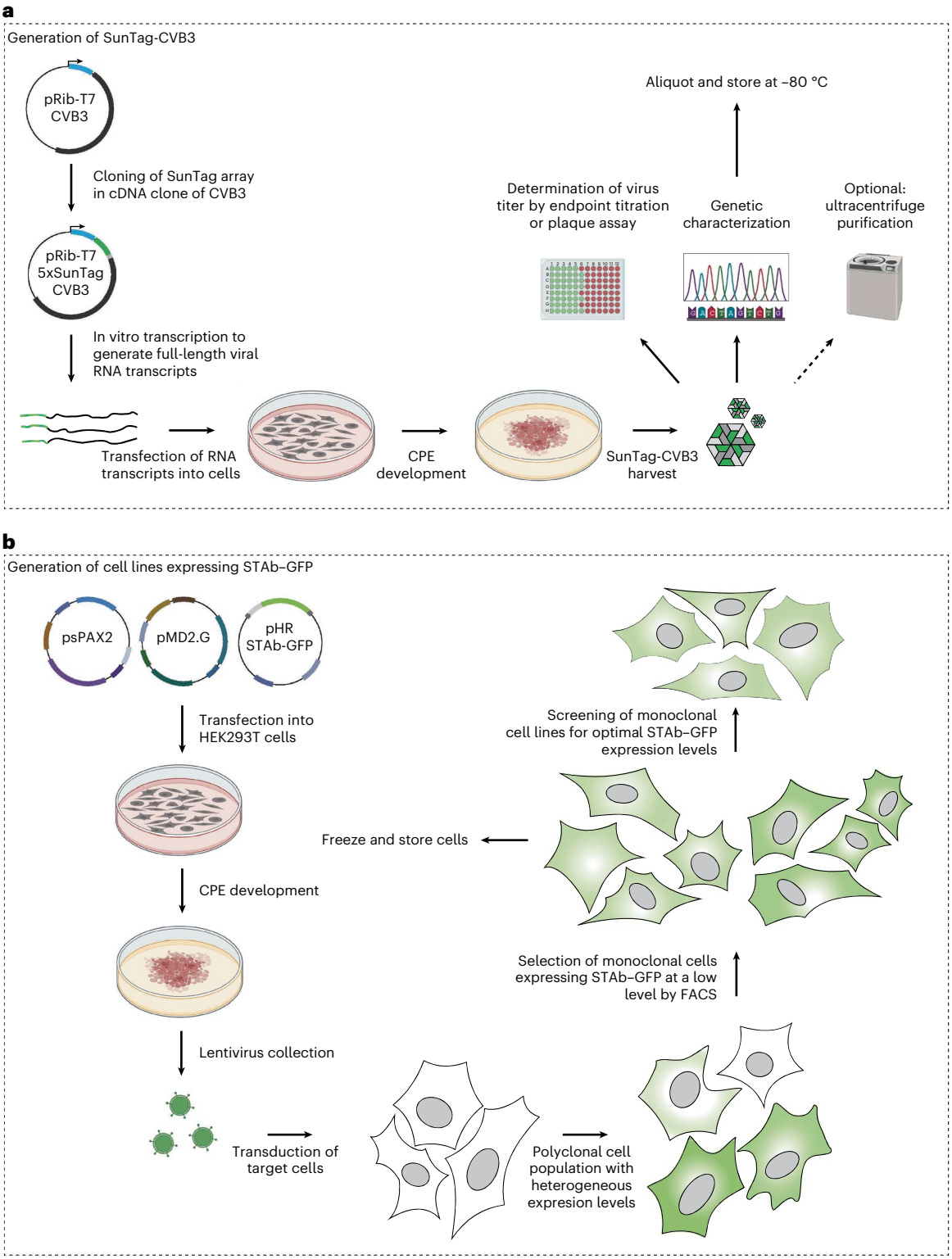

of the SunTag peptide array to a mature viral protein may interfere with the protein's function and thereby perturb viral fitness. Moreover, consider whether the (mature) protein to which the SunTag array is fused might accumulate in one or more locations in the cell, as such accumulation could lead to the appearance of fluorescent foci that appear similar to VIRIM foci

Fig. 4 | Workflow for generating SunTag-CVB3 virus and STAb–GFP expressing cell lines. a, A schematic workflow for producing and characterizing SunTag-CVB3 virus. The SunTag array is introduced in the plasmid carrying the cDNA copy of CVB3 via molecular cloning. Next, the full-length viral RNA runoff transcripts are generated by in vitro transcription. These are purified and transfected into producer cells (for example, HEK293T), which are monitored for the development of CPE, indicative of the virus replication. The appropriate negative controls should be included. Once CPE develops, the SunTag-CVB3 virus is collected, and viral RNA is isolated to check, by sequencing, whether the SunTag array was correctly inserted and maintained. Optionally, the stock can be purified and concentrated via ultracentrifugation. The viral titer is determined via endpoint titration or plaque assay. Finally, the stock is aliquoted and stored at −80 °C. **b**, A schematic workflow for generating cell lines expressing STAb–GFP. The lentivirus plasmid encoding STAb–GFP and packaging plasmids psPAX2 and pMD2.G are transfected into HEK293T cells, which are monitored for CPE development. Upon the observation of the full CPE, the supernatant containing the lentivirus is collected and purified. Optionally, the lentivirus stock can be titrated. Next, the target cells of interest are transduced with lentivirus and monitored for the expression of STAb–GFP. The resulting population of cells has heterogeneous expression levels of STAb–GFP. Next, these are sorted by FACS to isolate the monoclonal cells expressing STAb–GFP at a low level, which are subsequently grown out. These should be frozen and stored in liquid nitrogen or at −140 °C. Finally, the cells are screened functionally to find a clone with optimal expression levels of STAb–GFP. The figure was partly created in BioRender.com. Schipper, J. (2025) https://BioRender.com/ggk1n9j.

but that do not represent actively translated vRNAs. To circumvent these issues, we introduced a viral protease cleavage site between the SunTag repeats and the downstream viral protein. This protease cleavage site causes the release of the SunTag array from the viral polyprotein via proteolytic cleavage and ensures the functionality of the downstream viral protein (Fig. 2). Many viruses naturally encode a protease that may be employed in a similar fashion to minimize the impact of SunTag on viral protein function. Ideally, the protease only cleaves the SunTag peptides off from the polypeptide posttranslationally or after the ribosome has completed translation of the majority of the ORF to maximize the VIRIM foci brightness (Fig. 3). If no natural protease is available, a T2A site can be inserted in between the SunTag array and the downstream viral protein. Note, though, that a T2A site reduces the effective size of the ORF, reducing total VIRIM foci signal (Fig. 3).

Stage 2: virus production and characterization

Once the integration sites for the SunTag peptide array have been selected, the infectious virus needs to be produced and characterized. The exact procedure depends on the nature of the reverse genetics system that is available for the virus of interest. Here, we focus on the pRib-T7-CVB3-based reverse genetics system developed for CVB3 (Nancy strain), which has been described extensively before[73,74]. A schematic overview of the workflow outlined below for generating SunTag-CVB3 virus is depicted in Fig. 4a.

Generating a SunTag-virus infectious clone: the generation of SunTag-viruses starts with the molecular cloning of the SunTag array and possible additional genetic elements (for example, T2A sequences and cleavage sites) into the infectious cDNA plasmid of the virus. It is advisable to scramble the codon usage of the SunTag peptide array, such that each copy of the peptide uses different codons to encode the same amino acid sequence. The codon scrambling reduces the risk for genetic recombination during viral passaging. We recommend ordering a codon-scrambled SunTag array as a presynthesized DNA fragment to minimize the number of cloning steps and bypass the need for the PCR amplification of repetitive DNA sequences. The synthesized DNA fragments can be readily assembled into the linearized plasmid using commercially available kits such as NEBuilder HiFi DNA assembly (NEB). The resulting plasmids should always be carefully assessed for correct integration using PCR and sequencing. Moreover, for efficient downstream in vitro transcription reactions, the plasmid preparations should be properly purified and devoid of any (bacterial) contaminations or RNase.

Producing infectious viral RNA: after the correct plasmid has been cloned, the next step is to generate full-length infectious RNA copies of the viral genome, which can be transfected into susceptible producer cells to generate virus. To this end, an in vitro transcription reaction is set up using a T7-polymerase-based in vitro transcription kit (for example, Promega T7 RiboMAX Large Scale RNA Production System). First, the plasmid needs to be cut directly after the viral genome coding sequence to exclude any nonviral sequences from being included. For the pRib-T7-CVB3 plasmid, this is done using an MluI restriction digest. Next, the linearized DNA template is column-purified and used in the in vitro transcription reaction. Once the infectious RNA has been generated, the reaction mixture is treated with DNase to remove template

DNA. Finally, the infectious RNA should be checked by agarose gel for proper size and purity. Contamination with RNase will result in a smear instead of a clear band on the gel.

Transfection of infectious RNA: the purified infectious RNA can now be transfected into a cell line suitable for virus production. Here, several important points should be considered. First, the cell line used should be susceptible to infection by the virus or virus mutant. This is largely determined by the receptor tropism of the virus but might also be influenced by the cell-type-specific expression of restriction factors. Moreover, certain viruses—especially those with fitness-reducing mutations—are more susceptible to restriction factors or interferon signaling. Consequently, for these viruses, cell lines should be used that are defective in interferon production (for example, baby hamster kidney 21 (BHK-21) or African Green monkey Vero-E6 cells[75,76]). Another consideration is the amount of RNA to be transfected, as well as the number of cells and the culture container format. Owing to the stochastic nature of recombination, we have observed in the past that the insert might be (partially) deleted in a subset of the transfected wells. Such mutated genomes can be propagated when growing up the virus and contaminate the final viral stock. Consequently, depending on the expected difficulty in maintaining the desired inserts (based on size, insert location and so on), transfections might be pursued in multiple distinct wells or containers in parallel. For 5xSunTag-CVB3, we seed HEK293T cells in T75 culture flasks at 50–70% confluency on the day of transfection. We transfect 5 µg of RNA using Lipofectamine 2000, but other transfection reagents should work as well. It is important to include appropriate controls (that is, transfection controls and transfection of wild-type virus RNA). Next, cells are incubated and, depending on the nature of the virus, monitored for the development of cytopathogenic effect (CPE).

Recovery and characterization of virus: once the full CPE is observed, the virus-containing supernatant is collected, cleared of cellular debris and characterized. The viral characterization includes viral RNA isolation and a subsequent reverse-transcription reaction to generate cDNA. From this cDNA, the desired viral sequences can be amplified by PCR and checked by agarose gel and sequencing to assess whether the SunTag array was properly maintained in the viral genome. We typically design primers between 18 and 25 nucleotides in length with a GC content between 40% and 60%, a 3′-terminal G or C and a melting temperature between 55 °C and 65 °C. Make sure that primers are specific (that is, that they do not have additional off-target binding sites), do not form secondary structures and do not form primer dimers (that is, have too high a degree of complementarity to each other). We typically use commercial software (for example, Snapgene) to aid in the primer design and molecular cloning. After the initial successful recovery of SunTag-virus, it can be passaged onto fresh monolayers of susceptible cells to produce larger amounts of viruses (which is termed passage 1 or P1). This should always be done at low multiplicity of infection (MOI) as to limit the probability of defective interfering virus formation. The P1 stock is checked in the same way as described above. Optionally, stocks can be subjected to sucrose-cushion ultracentrifugation to remove any impurities and enhance virus concentrations. Finally, the stocks should be titrated using either 50% tissue culture infectious dose ($TCID_{50}$) or plaque assay[77–80]. Importantly, the initial VIRIM experiments should always include a range of dilutions to find the optimal dilution of virus to effectively reach the desired fraction of infected cells appropriate for the experiment at hand. Owing to different experimental and infection conditions between single-cycle VIRIM experiments and endpoint titrations, the dilution to be used might differ somewhat from the theoretical dilution based on endpoint titration.

Stage 3: generation of reporter cell lines

Host cell type: a key component of the VIRIM assay is the host cell line that stably expresses the STAb–GFP. In principle, any cell type that can be transfected or transduced with (lenti-) viruses to stably express the STAb is amenable to VIRIM experiments. We have successfully generated STAb–GFP-expressing cell lines in commonly used cell types, such as U2OS, HeLa and A549. In addition, we have established STAb–GFP-expressing small intestinal organoid cultures, enabling VIRIM to be carried out in an untransformed system with heterogeneous cell types. When selecting a cell type for VIRIM experiments, it is also important to consider how suitable the cells are for high resolution imaging. Relatively flat, adherent and large cells are more

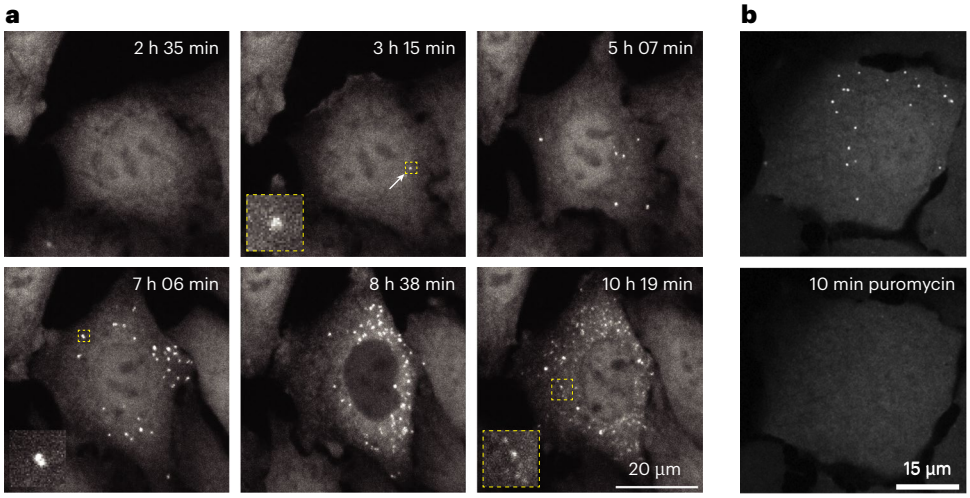

Fig. 5 | Example images of STAb–GFP expressing cells and the VIRIM assay. a, The monoclonal HeLa cell line expressing STAb–GFP (AausFP1) at optimal levels for long-term VIRIM imaging, infected with SunTag-CVB3 and imaged at different timepoints after infection. The yellow dotted lines indicate areas of zoom. As the infection progresses, the number of VIRIM foci increases. Rapid movement of the translating vRNA during image acquisition can result in a slight shift in the location of the spot in different *Z*-slices. Bottom left zoom, white arrows: In a maximum intensity projection image, this results in what appears to be a second VIRIM focus directly adjacent to the main spot. These can usually be distinguished from two bona fide VIRIM foci that are in close vicinity to each other by looking at the frames prior and after, which should have only one spot. Bottom middle: the initial stages of STAb–GFP depletion can be recognized by the diffusion of nuclear STAb–GFP to the cytosol. Bottom right: Finally, upon antibody depletion, the binding stoichiometry of STAb–GFP to new SunTag peptide arrays arising from actively translating vRNAs changes, resulting in dimmer VIRIM foci. **b**, A control experiment to show that VIRIM foci represent sites of active translation. Upon the addition of the translation inhibitor puromycin, VIRIM foci rapidly disappear. HeLa STAb–GFP reporter cells were infected with 5xSunTag-CVB3 and imaged at 2 h after infection. Subsequently, the cells were treated with puromycin (0.1 mg/ml) for 10 min and imaged again. The images in **b** were adapted with permission from ref. 2, Elsevier.

favorable than columnar or smaller cells or cells that are grown in suspension, because fewer *Z*-slices are needed during imaging to capture the entire cell volume. A schematic overview of the workflow for generating the reporter cell lines is given in Fig. 4b.

STAb–GFP expression levels: the expression levels of STAb–GFP in the reporter cell line are crucial for a successful VIRIM experiment. An example of a HeLa reporter cell line with STAb–GFP expression optimized for long-term VIRIM imaging assays with picornaviruses is depicted in Fig. 5a. Clearly defined diffraction-limited spots can be observed upon the infection of this cell line with SunTag-CVB3. The expression has been balanced to enable a good signal-to-noise ratio, with a long enough window before antibody depletion (Fig. 5a, bottom middle and right) sets in to allow the examination of the initial phases of replication and translation of enterovirus infection. If expression levels are too low, not all SunTag epitopes will be bound by STAb–GFP, resulting in low VIRIM spot intensity, precluding their reliable detection. These foci would resemble the lower intensity foci observed at late timepoints after infection in this cell line when STAb–GFP has been depleted (Fig. 5a, bottom right). By contrast, high expression levels will result in higher background fluorescence and a decreased signal-to-noise ratio. The exact fluorescent protein attached to the STAb is also important. Using brighter will provide brighter VIRIM foci, but additionally, several induce the aggregation of the STAb[41]. We typically use AausFP1, a very bright green fluorescent protein[81], which works well as a fusion with the STAb. In practice, the lentiviral transduction protocol will result in cells with heterogeneous STAb expression levels. Even though these polyclonal cells can be directly used for VIRIM imaging experiments, to provide consistency between cells and mitigate any potential effects of differing STAb–GFP expression levels on assay readouts, we strongly suggest making monoclonal cell lines with homogeneous expression levels. We typically generate monoclonal cell lines with a range of expression levels and screen clones using VIRIM for optimal signal-to-noise ratios and antibody

depletion rates for the virus and conditions specific to the assay. Typically, we express STAb–GFP under the control of an attenuated promoter and isolate the lowest STAb–GFP expressing cells (~bottom 25%) by FACS for making monoclonal cell lines.

Stage 4: imaging infections

We perform our VIRIM experiments using a temperature-controlled spinning disk confocal microscope equipped with a highly sensitive sCMOS camera (Photometrics Prime 95B). This setup combines high sensitivity, fast image acquisition and low light-induced toxicity, which enables the detection of fast-moving and relatively dim VIRIM foci in live cells. Point-scanning confocal microscopes may also work if coupled to a highly sensitive detector, but they typically require longer acquisition times and may therefore limit the temporal resolution that can be achieved. Widefield microscopy could also be attempted but will probably create higher background signal compared to confocal imaging owing to light pollution from out-of-focus *Z*-planes.

We have successfully imaged CVB3 viral translation sites using 40×, 60× and 100× magnification objectives using a numerical aperture (NA) of at least 1.4. In general, lower magnification (40×) allows the imaging of more cells in a single field of view and therefore generates more data in a single experiment. Higher magnification (100×) provides increased spatial resolution and is therefore used, for instance, for determining the diffusive properties of individual VIRIM foci. Of note, the magnification per se does not affect the ability to detect a translating vRNA, as the VIRIM signal is detected as a diffraction-limited spot at all magnifications. Instead, the NA of the objective is important, because it determines the amount of fluorescence signal that can be collected, with higher NA values allowing the capture of more signal. Importantly, objectives also have different working distances, with higher magnification objectives typically having lower working distances. When performing VIRIM on confluent monolayers, working distances are generally not limiting, but the imaging of thicker three-dimensional (3D) cell cultures (for example, small intestinal organoid cultures) may require the use of objectives with longer working distances.

Depending on the goal of the experiment, a VIRIM experiment may require a total imaging time ranging from a few minutes (for example, to determine vRNA mobility) to multiple hours (for example, to determine replication rates). The acquisition laser power, exposure time and imaging time interval should be optimized to minimize fluorophore bleaching and phototoxicity, while maintaining sufficient signal to detect VIRIM foci at a frame rate that captures the relevant biological process. We typically acquire images at 3–15-min time intervals to study viral infection progression. In addition, translating vRNAs are present throughout the entire cytoplasm, requiring the acquisition of multiple *Z*-slices to cover the complete cell volume.

Depending on the goal of the experiment, an appropriate MOI/virus dilution should be chosen. As mentioned earlier, in VIRIM experiments where you use a new virus stock, it is advisable to include a range of virus dilutions to identify an optimal MOI.

As a control to ascertain whether fluorescent foci indeed reflect vRNAs being actively translated, cells can be treated with puromycin, an inhibitor of translation, which should result in the rapid (<1 min) disappearance of VIRIM foci (Fig. 5b). Moreover, cells can be treated with viral replication inhibitors, which should inhibit the increase in the number of VIRIM foci over time.

Finally, certain VIRIM experiments might involve the use of drugs or other treatments to examine the role of host or viral factors on early viral infection dynamic. Examples of this include pretreatment with cytokines, chemical inhibition of host or viral factors and transient depletion or upregulation of host factors (for example, via RNA interference). Depending on the exact nature of the experiment, this might require pretreatment or conditioning of STAb–GFP-expressing cells with the compound of interest. Moreover, sometimes the compound needs to be included in the imaging medium.

Stage 5: image processing and data analysis

The careful analysis of the acquired microscopy data is necessary to derive biological insights from a VIRIM experiment. Typical VIRIM analyses involve counting the number of VIRIM foci, determining the fluorescence intensity of VIRIM foci and spatial tracking of individual foci.

These parameters can be used to study early infection progression, viral translation efficiency, replication rates and the diffusive properties of translating vRNAs, respectively. It is important to set clear criteria for the inclusion and exclusion of particular infected cells to prevent biases in the analysis. For example, depending on the desired parameters to be analyzed, one might want to exclude cells that undergo cell division during the imaging experiment, cells which migrate (partly) out of the field of view during the recording, infections that start after a certain timepoint in the recording, cells that are infected by multiple viruses at once, cells where infection has started before the start of recording, cells where follow-up time from start of infection is short, cells that die early during infection and so on. To avoid any potential bias, it is pivotal to set these criteria beforehand and apply them consistently across samples.

Counting VIRIM foci and assigning 'infection phases': to follow viral infection progression using VIRIM, the number of VIRIM foci can be scored over time. For picornaviruses, we have previously identified distinct infection phases for which the duration and/or the successful completion can be scored and compared between different conditions (for example, host factor knockout or pharmacological inhibition). We demonstrated that these infection phases reflect sequential, coordinated cycles of vRNA translation and replication. When using a low MOI, infections typically start with a single vRNA per cell, represented by a single VIRIM spot, which we refer to as infection phase 1. At the onset of replication, vRNA translation is halted, resulting in the disappearance of the VIRIM spot, which marks the start of infection phase 2: initial replication. When the translation of the newly synthesized vRNAs is initiated, a reappearance and subsequent rapid increase in the number of VIRIM foci is observed (infection phase 3). For CVB3, typically ~15–20 new VIRIM foci appear during phase 3, after which, the new synthesis of vRNAs stops and the number of new VIRIM foci remains constant, marking the start of infection phase 4. Finally, a new second burst of VIRIM foci is observed (~1 h after the start of phase 4 for CVB3), reflecting a second cycle of vRNA replication and marking the start of infection phase 5. Precisely assigning an infection phase in a time-lapse movie can difficult because of technical noise in capturing and counting VIRIM foci, resulting in variable numbers of VIRIM foci over time. In the procedure, we provide practical guidelines for the assignment of infection phases for CVB3 in the light of such variation, and these guidelines may serve as an example to establish similar infection phases for other viruses as well (Box 1).

Extracting vRNA translation efficiency values from VIRIM foci intensities: it is possible to extract quantitative information on vRNA translation efficiency from the intensity of VIRIM foci. However, such analysis requires careful quantification and a good understanding of the underlying biological process and assay design.

The fluorescent signal originating from a VIRIM spot is dependent on the number of nascent polypeptide chains associated with the vRNA at any given moment. As such, the intensity of VIRIM foci reports on the translation efficiency of the translating vRNA. Translation efficiencies of vRNAs can be compared between different locations in the cell, or during different times in infection. Extracting intensity features (for example, VIRIM spot intensity) from a time-lapse microscopy experiment requires image corrections, such as bleach correction and flat-field correction, before the intensity measurement. Furthermore, it is important to realize that the fluorescence intensity of a single translating vRNA is dynamic, as ribosome loading onto vRNAs is probably stochastic, with variable numbers of ribosomes per vRNA between vRNA molecules and for single vRNAs over time. To compare viral translation site intensities between conditions (for example, wild-type versus mutant virus) it is therefore necessary to measure the intensity of many VIRIM foci (>200 foci) to average out stochasticity that is inherent to translation.

VIRIM spot intensity can also provide information on the absolute number of ribosomes loaded on the vRNA. For this, it is necessary to measure the fluorescence intensity of a single mature SunTag peptide/STAb–GFP complex. By dividing the fluorescence intensity of the viral translation site by the intensity of a single SunTag peptide/STAb–GFP complex (and correcting for partially translated SunTag arrays) the number of nascent chains and therefore the number of ribosomes on the viral RNA can be determined (see ref. 46 for more details).

vRNA mobility: to determine the mobility of translating vRNAs, individual VIRIM foci need to be tracked over time. The ability to track single VIRIM foci depends on the number of foci in the cell, their speed of movement and the time interval between frames. Although 3D spot

BOX 1

Assigning VIRIM infection phases based on the number of viral translation sites

Using VIRIM for the picornaviruses CVB3 and EMCV, we observed a recurrent pattern in the appearance and disappearance of viral translation sites. We termed the individual steps in this pattern VIRIM infection phases and demonstrated that these phases originate from alternating cycles of translation and replication of the viral RNA (Fig. 6a,b). Note that the duration of such infection phases might differ considerably for different viruses. To determine the duration of VIRIM infection phases, it is necessary to assign a VIRIM infection phase to each time frame. The following guidelines were used for this.

Assigning VIRIM phase 1 and 2: the initial appearance of a VIRIM spot after virus inoculum addition marks the start of VIRIM phase 1 and reflects the initial translation of the incoming vRNA. During phase one, some timepoints may not have a detectable VIRIM spot as a result of spot mobility or technical noise. If a translation site is absent in one timepoint (at maximum 5 min interval) and then reappears, it is still assigned to VIRIM phase 1 (we determined the phase 1 calling accuracy in our experiments and found that in more than 90% of all timepoints assigned to phase 1, exactly one viral translation site was detected).

Phase 1 ends when the initial translation site disappears and remains absent for at least three timepoints (at 3–5-min interval between timepoints). The phase 1 duration is highly heterogeneous and lasts from 12 min up to 4 h. As soon as the spot has disappeared from at least three timepoints, VIRIM phase 2 has initiated, during which the incoming vRNA is replicated. The three-timeframe threshold for assigning phase 2 was based on the observation that phase 1 spots are rarely missed in more than two consecutive frames.

Phase 2 can end in three different ways. Successful replication is marked by the reappearance of multiple VIRIM spots, indicating the start of phase 3. However, in a subset of infections, replication is not successful. This can result either in a complete arrest of the infection, with no reappearance of any spots (termed phase 2 arrest or stalled infection), or in a reinitiation of translation of the original incoming vRNA, marked by the reappearance of a single VIRIM spot. In the latter situation, renewed entry into phase 2 may be observed at a later timepoint. The pattern of alternating replication and reinitiation of translation can reoccur multiple times, and these are termed translation 'pulses' and replication 'breaks' (Fig. 6c). Many of these infections will eventually result in successful replication and the start of phase 3.

Assigning VIRIM phase 3–5: if replication is successful, phase 3 starts with the reappearance and rapid increase in the number of VIRIM foci after the absence of viral translation during phase 2. The appearance of multiple viral translation sites reflects initiation of viral translation of newly synthesized vRNAs and therefore signifies successful replication of the incoming viral genome. After an initial increase in the number of viral translation sites, a period during which the number of VIRIM foci remains stable or even slightly decreases marks VIRIM phase 4. During this phase, there is continued translation, but no new vRNAs are synthesized that engage in translation. A second round of viral replication takes place near the end of phase 4. Upon the initiation of translation on the resultant new vRNAs, a further increase in the number of VIRIM foci can be observed. This second burst of viral translation is defined as the start of VIRIM phase 5. Phases 2–4 have quite constant durations[2] (approximately as follows: phase 2: ~15–45 min; phase 3: ~15–60 min; phase 4: ~15–60 min), with much less heterogeneity than the phase 1 duration.

Although defining the start of VIRIM phase 3 is relatively straightforward, pinpointing the start and end of phase 4 can be more challenging. Plotting a moving average of the number of VIRIM foci may help to define when the number of VIRIM foci reaches a plateau (start of phase 4) and when the number starts increasing again after reaching a plateau (start of phase 5). Similar to phase 2, we defined a minimum duration of 12.5 min for VIRIM phase 4.

tracking can be performed, we typically image only a single *Z*-plane or process the *Z*-stack images to generate maximum intensity projections and perform downstream analysis on the two-dimensional images. ImageJ provides several plugins that combine automated spot detection with a tracking algorithm (for example, TrackMate[82]). These can be used to generate a series of *x*,*y* coordinates for the individual VIRIM foci that can be used to calculate the mean squared displacement (MSD), which can provide insights into the diffusive properties of the translating vRNA.

Materials

Biological materials

Cells

- Reporter cell line: in the original study describing the VIRIM technology, U2OS cells were mostly used (American Type Culture Collection (ATCC), cat. no. HTB-96, Research Resource

Identifier (RRID): CVCL_0042), but we have successfully applied VIRIM in several other cell types as well (for example, HeLa cells and intestinal organoids)
- Lentivirus production cell line: HEK293T cells (ATCC, cat. no. CRL-3216, RRID: CVCL_0063)
- Picornavirus production cell lines: HEK293T cells (see above), BHK-21 C13 (ATCC, cat. no. CCL-10, RRID: CVCL_1915), Vero-E6 (ATCC, cat. no. CRL-1586, RRID: CVCL_0574)
  ▲ **CAUTION** Ensure that cell lines are verified and devoid of mycoplasma contamination and lentiviruses.
- Virus CVB3, strain Nancy. Genbank accession number: JX312064.1
  ▲ **CAUTION** Work involving CVB3 should only be performed in biosafety level 2 labs or higher with appropriate personal protection by persons that are adequately trained. Working with genetically engineered CVB3 may require government authorization, for which conditions and regulations may vary between countries.

Plasmids
- pRib-T7-CVB3 reverse genetics system for CVB3 (Nancy strain)[73,74]
- Lentiviral plasmid encoding STAb–GFP (Addgene plasmid 60907)
- Helper plasmids for lentivirus production; psPAX2 (Addgene plasmid 12260) and pMD2.G (Addgene plasmid 12259)

Reagents
- Dulbecco's modified Eagle medium (DMEM; Thermo Fisher Scientific, cat. no. 31966021)
- Fetal calf serum (FCS; Thermo Fisher Scientific, cat. no. F7524)
- Penicillin–streptomycin (Thermo Fisher Scientific, cat. no. 15140-122)
- Dulbecco's phosphate-buffered saline (DPBS), without Ca^{2+}/Mg^{2+} (Capricorn Scientific, cat. no. PBS-1A)
- Optimized minimal essential medium (reduced-serum medium) (Opti-MEM; Thermo Fisher Scientific, cat. no. 11058021).
- Fugene (Promega, cat. no. E231A)
- Lipofectamine 2000 (Thermo Fisher Scientific, cat. no. 11668027)
- Leibovitz's L15 medium (Thermo Fisher Scientific, cat. no. 21083-027), supplemented with 5% FCS and 1% penicillin–streptomycin
- Puromycin (Thermo Fisher Scientific, cat. no. 12122530)
  ▲ **CAUTION** Puromycin is harmful. Wear gloves and avoid contact with eyes and skin.
- MluI-HF restriction enzyme (New England Biolabs, cat. no. R3198S)
- 10× rCutsmart buffer (New England Biolabs, cat. no. B6004S)
- Tris–acetate–ethylenediaminetetraacetic acid buffer (10×), RNase-free (Thermo Fisher Scientific, Invitrogen, cat. no. AM9869)
- Midori Green Advance DNA/RNA stain (NIPPON Genetics, cat. no. MG04)
- Gel loading dye, purple (6×) (New England Biolabs, cat. no. B7024S)
- RNA Gel Loading dye (2×) (Thermo Fisher Scientific, cat. no. R0641)
- UltraPure Agarose (Thermo Fisher Scientific, Invitrogen, cat. no. 16500500)
- GeneRuler DNA ladder mix (Thermo Fisher Scientific, cat. no. SM0332)
- RiboMAX Large Scale RNA production System—T7 (Promega, cat. no. P1300)
- NucleoSpin RNA virus, mini kit for viral RNA from cell-free fluids (Macherey-Nagel, cat. no. 740956.50)
- NucleoBond Xtra, Midi kit for transfection-grade plasmid DNA (Macherey-Nagel, cat. no. 740410.50)
- NucleoSpin RNA, Mini kit for RNA purification (Macherey-Nagel, cat. no. 740955.50)
- NucleoSpin Gel and PCR clean-up, mini kit for gel extraction or PCR clean-up (Macherey-Nagel, cat. no. 740609.50)
- Superscript III reverse transcriptase kit (Thermo Fisher Scientific, Invitrogen, cat. no. 18080093)
- Random hexamer primers (Thermo Fisher Scientific, Invitrogen, cat. no. N8080127)
- RNase inhibitor (Thermo Fisher Scientific, Invitrogen, cat. no. N8080119)
- Q5 High-Fidelity DNA polymerase (New England Biolabs, cat. no. M0491S)

- Equimolar mix of deoxynucleotide triphosphate (dNTP) (Promega cat. nos. U1205/ U1215/ U1225/U1235)
- NEBuilder HiFi DNA assembly cloning kit (New England Biolabs, cat. no. E5520S)
- RNase-free H_2O (diethyl pyrocarbonate (DEPC)-treated) (Merck, cat. no. 593520-1L)
- RiboLock RNase inhibitor (Thermo Fisher Scientific, cat. no. EO0381)
- Atto-488-NHS ester (Atto-Tec GmbH, cat. no. AD 488-31)
- Sodium hydroxide (NaOH) pellets (Merck, cat. no. 106498)

Equipment

- 5-ml Luer-lock disposable syringe (BD, cat. no. 309646)
- 0.45-µm syringe filter (Carl Roth, cat. no. KH55.1)
- 15-ml conical tube (CellStar, Greiner Bio-One, cat. no. 188271)
- 50-ml conical tube (CellStar, Greiner Bio-One, cat. no. 227261)
- 10-cm tissue culture plate (CellStar, Greiner Bio-One, cat. no. 664160)
- 25-cm^2/75-cm^2/175-cm^2 cell culture filter cap flasks (CellStar, Greiner Bio-One, cat. nos. 690175, 658175 and 660175)
- 1.5-ml Eppendorf tubes (Eppendorf, cat. no. 0030123611)
- 96-well flat-bottom plate (CellStar, Greiner Bio-One, cat. no. 655180)
- 96-well glass-bottom plate (Ibidi, cat. no. 89627)
- 200-µl PCR tubes (SARSTEDT, cat. no. 72.991.002)
- Optional for ultracentrifugation: 38.5 ml, Open-Top Thinwall Ultra-Clear Tubes, 25 mm × 89 mm (Beckman-Coulter, cat. no. 344058)
- Cell culture incubator (37 °C, 5% CO_2, humidified) (Panasonic, model no. MCO-170AICUVH-PE)
- Flow cytometry system (BD, model no. FACS Aria II)
- Confocal spinning disk microscope system (see 'Imaging infections' section of Experimental Design for hardware requirements). We use a Nikon TI2 inverted microscope equipped with a CSU-X1 spinning disk (Yokogawa), Prime 95b sCMOS camera (Photometrics, cat. no. 01-PRIME-95B-R-M-16-C), 60× 1.45 NA objective, perfect-focus system and a temperature-controlled incubator
- Thermal cycler for polymerase chain reaction (PCR) (for example, T100 Thermal cycler; Bio-rad, cat. no. 1861096)
- Equipment for running agarose gels (for example, Mini-Sub Cell GT Horizontal Electrophoresis System, 7 × 7 cm tray, with casting gates; Bio-rad, cat. no. 1704406)
- UV–visible spectrophotometer for measuring DNA and RNA concentrations (for example, NanoDrop Ultra microvolume UV-vis spectrophotometer; Thermo Fisher Scientific, cat. no. NDULTRACFLGL)
- Temperature-controlled centrifuges for small (that is, 1.5 ml/2 ml) (for example, Eppendorf 5425R, cat. no. EP5406000119) and larger tubes (that is, 15 ml/50 ml) (for example, Multifuge X1R Pro, cat. no. 75009750)
- Temperature-controlled incubators for bacterial culture (shaking incubator and plate incubator) (for example, MaxQ 6000 shaking incubator, cat. no. SHKE6000-1CE)
- Optional: ultracentrifuge. We use either a Beckman-Coulter Optima L-90K (production discontinued) or Optima XE-90 (cat. no. A94471) with SW-32-Ti swinging bucket rotor (cat. no. 369650)

Software

- NIS-Elements software for microscope control
- ImageJ https://imagej.net/ij/
- MATLAB (MathWorks: https://nl.mathworks.com/products/matlab.html)
- Snapgene https://www.snapgene.com/

Reagents setup

- Complete media (both DMEM and Leibovitz's L15) are created by the addition of 5% FCS and 1% penicillin–streptomycin. Complete media should be stored at 4 °C and can be used for ~4 months

Procedure

Stage 1: design of SunTag-virus and molecular cloning to obtain infectious cDNA plasmid

● **TIMING 5–10 days**

Design of SunTag-virus

1. Identify sites in the viral genome to insert an array of SunTag peptide epitopes in the viral coding sequence using the general strategy outlined in the 'Experimental design' section.

Molecular cloning to obtain the infectious clone plasmid of SunTag-virus

1. Identify sites in the viral genome to insert an array of SunTag peptide epitopes in the viral coding sequence using the general strategy outlined in the 'Experimental design' section.
2. Use a preferred molecular cloning approach to generate one or more plasmids encoding the modified viral genome that can subsequently be used for the production of the SunTag-virus.
   ▲ **CRITICAL STEP** As outlined in the 'Experimental design' section, it is advisable to order codon-scrambled SunTag arrays that include additional elements (for example, protease cleavage sites or T2A sequences) as presynthesized DNA fragments that can be readily assembled into the backbone plasmid.
3. Purify the plasmids from the bacterial cultures using the midi-prep DNA isolation kit, following the manufacturer's instructions.
4. Determine the concentration and purity using the UV–visible spectrophotometer. The next steps require at least 5 µg of plasmid DNA. Assess the purity by looking at the A260:A280 and A230:A260 ratios, which report on contaminations with protein and chemicals, lipids or salts, respectively. An A260:A280 ratio of 1.8–2.0 and an A230:A260 of 2.0–2.2 are considered pure.
5. Confirm that the SunTag array is correctly inserted in the plasmid by sequencing, for which we use a commercial vendor.

Stage 2: 5xSunTag-CVB3 production and characterization

● **TIMING 5–10 days**

In vitro transcription reaction

▲ **CRITICAL** From here onwards, work RNase-free (that is, use gloves, decontaminate surfaces, use RNase-free tips and reagents and so on).

6. In a 1.5-ml tube, set up a restriction digestion reaction to linearize 1–5 µg of pRib-T7-5xSunTag-CVB3 plasmid with MluI according to manufacturer's instructions.
7. Run the entire digestion reaction on agarose gel. For reference, load a lane with 50–100 ng undigested plasmid. We typically use 1% agarose in 1× Tris–acetate–ethylenediaminetetraacetic acid buffer with Midori Green Advance DNA/RNA stain and run at 100 V for 30–45 min until the running front has reached the end of the gel. The linearized plasmid should run lower in the gel than the undigested plasmid. Column-purify from gel using PCR/Gel clean-up kit, following the manufacturer's instructions. Determine the concentration using UV–visible spectrophotometry.
8. Set up the following in vitro transcription reaction in a PCR tube and incubate at 37 °C for 2 h.

Component	Amount
Linearized DNA template	400 ng
T7 polymerase enzyme mix (RiboMAX)	4 µl
T7 buffer 5× (RiboMAX)	10 µl
Ribonucleotide triphosphate mix (RiboMAX)	10 µl
RNase-free water	Up to 50 µl

9. Add 1 µl RNase-free DNase (RiboMAX) and incubate at 37 °C for 30 min to digest DNA template.
10. Purify RNA using RNA purification columns (NucleoSpin, Macherey-Nagel) following the manufacturer's instructions and measure concentration using a UV–visible photospectrometer set for RNA measurement. In total, 25–50 µg of RNA yield can generally be expected.
    ◆ **TROUBLESHOOTING**

11. Prepare an RNase-free 1% agarose gel. Use fresh and RNase-free reagents. We decontaminate gel (casting) equipment by treating with 0.2M NaOH for 30 min. Afterward, rinse thoroughly with RNase-free water to get rid of any residual NaOH. Load 1–3 µg of RNA in RNA gel loading dye and run at 100 V for 30–45 min. Here, it is important to see a sharp band and not a smear, which might indicate RNase contamination.
◆ **TROUBLESHOOTING**
12. Store the infectious RNA at −80 °C.
■ **PAUSE POINT** Infectious RNA can be stored indefinitely at −80 °C. Avoid repeated freeze–thaw cycles.

Transfection of infectious RNA into virus producer cells

13. Seed HEK293T cells in a T75 tissue culture flask so that they reach 50–70% confluency on the next day. In our experience, this is achieved by seeding ~3.0–5.0 million cells in 10 ml of complete DMEM.
14. The next day, check cells by light microscopy for appropriate confluency.
▲ **CRITICAL STEP** Low cellular density may severely impact the virus yield.
15. To transfect cells with the infectious RNA, we typically use Lipofectamine 2000 at a 1:1 ratio, following the manufacturer's protocol. First, for each flask of cells to be transfected, prepare 5 µg of infectious RNA (from Step 12) in 250-µl Opti-MEM medium and gently mix by pipetting.
▲ **CRITICAL STEP** Include both a positive control (infectious RNA of the wild-type virus) to check whether the procedure itself succeeded and a negative control (empty transfection) to assess any possible cellular toxicity unrelated to production of the virus (for example, owing to transfection itself). These can be scaled down in volume to save reagents.
16. In a separate tube, add for each flask to be transfected 5 µl of lipofectamine to 250 µl of opti-MEM and gently mix by pipetting.
17. After 5 min of incubation at room temperature (on average, 20 °C in our laboratory), gently mix both solutions together at a 1:1 ratio for a total volume of 500 µl for each flask to be transfected. Incubate for 15–20 min at room temperature.
18. Add 500 µl of the transfection mix to each flask. We do not remove cell culture medium (DMEM + 10% FCS) beforehand or change medium after the initial incubation with transfection mix, although this might enhance transfection efficiency somewhat (depending on the reagents and cells used). Make sure to spread the transfection mix out over the flask by gently rocking the flask back and forth.
▲ **CAUTION** From here on flasks should be handled in appropriate biosafety level laboratories (that is, BSL-2 for CVB3).
19. Incubate the flasks at 37 °C and regularly monitor the cells by microscope for the development of CPE. For CVB3, CPE can be recognized distinctly as cells rounding up, eventually progressing to cell death and detachment. Typically, distinct foci within the monolayer where CPE starts to develop can be distinguished macroscopically. The relative speed at which CPE develops compared with wild-type virus control can often already give an indication of the impact of genetic inserts (that is, the SunTag array) on viral replicative fitness.
◆ **TROUBLESHOOTING**

Recovery and characterization of virus

20. When CPE reaches >90% (that is, most cells have died and detached), any remaining cells can be disrupted by two to three cycles of freeze–thawing at −80 °C. Ensure that the flasks freeze and thaw completely before repeating. Place flasks in plastic bags and thaw in an appropriate biosafety hood as the plastic of the flasks might crack during freeze–thawing.
▲ **CRITICAL STEP** Note that freeze–thaw cycles might be detrimental to viral yield for enveloped viruses.
■ **PAUSE POINT** Flasks can be stored at −80 °C during this stage indefinitely.
21. Transfer the entire supernatant to a 15-ml centrifuge tube and centrifuge for 5 min at 400*g* at room temperature. Transfer the virus-containing supernatant to fresh tubes. Store at −80 °C.
■ **PAUSE POINT** The virus-containing supernatant can be stored at −80 °C during this stage indefinitely.

▲ **CRITICAL STEP** It is advisable to aliquot the stocks before freezing, especially for viruses that are sensitive to repeated freeze–thaw cycles. However, the stock should be stored collectively if optional ultracentrifugation step is pursued later (Steps 31–38).

22. Next, to assess whether the viruses maintained the inserts, the viral RNA needs to be isolated. Use a commercially available spin-column isolation kit specific for viral RNA ('Materials' section), following the manufacturer's instructions.
▲ **CRITICAL STEP** Once the viral RNA is obtained, it should be kept on ice at all times.
23. Once the viral RNA is isolated, set up a reverse-transcription reaction to generate a cDNA copy using the SuperScript-III reverse transcription kit with random hexamer primers, following the manufacturer's instructions. First, add 5 µl of the RNA sample from Step 22 to a PCR tube with 5.75 µl of RNase-free H_2O and 1.25 µl of random hexamers (50 µM). Mix and incubate for 5 min at 65 °C in a heating block or PCR machine. Place on ice for 1 min, spin briefly and place on ice again.
24. Keep the tube on ice and add 5 µl of first strand buffer (5×), 1 µl of dNTP mix, 1 µl of dithiothreitol (DTT) (0.1 µM), 1 µl of RNAse inhibitor, 1 µl of SuperScript-III reverse transcriptase (200 U/µl) and 4 µl of RNase-free H_2O (total volume 25 µl).
25. Place in the thermal cycler and run the following program:

Time	Temperature
5 min	25 °C
30–60 min	50 °C
5 min	85 °C

■ **PAUSE POINT** The cDNA can be stored at −20 °C indefinitely, or directly proceed to PCR.

26. Next, set up a PCR reaction with primers specifically designed to amplify the regions of interest (ROIs) (for example, the SunTag sequence) following the manufacturer's instructions for the Q5-polymerase. Preferably design primers in such a way that it is easy to ascertain on agarose gel whether the insert was maintained in the viral genome. It is also advisable for easy reference to run positive control PCR reactions using the original infectious cDNA plasmid clones from stage 1. Prepare the master mix as follows:

Component	Volume for 1× reaction
H_2O	28.5 µl
5× Q5 buffer	10 µl
Forward primer (10 µM)	2.5 µl
Reverse primer (10 µM)	2.5 µl
dNTP mix (10 mM each)	1 µl
Q5 DNA polymerase	0.5 µl

27. Add 5 µl of each viral cDNA copy (from Step 25) or control plasmid (that is, the original cDNA infectious clone plasmids from stage 1) (25 ng in 5 µl H_2O or TE buffer) and 45 µl master mix to a PCR tube.
28. Place the tubes in a thermal cycler and run the following protocol:

Temperature	Time	
98 °C	30 s	
98 °C	10 s	
65 °C[a]	20 s	35 cycles
72 °C	1 min[b]	
72 °C	5 min	
4 °C	Infinite hold	

[a]Depends on melting temperature of primers. [b]Depends on length of amplicon (elongation rate of Q5-polymerase is ~40 s/kb).

■ **PAUSE POINT** PCR products can be stored at −20 °C for several months up to 1 year.

29. Mix 10 µl of the PCR reaction with 2 µl 6× loading buffer and load 10 µl on a 1% agarose gel. Run for 30–45 min at 100 V. To ascertain whether the SunTag array was maintained in the virus, check if the PCR product from the virus sample runs at the same height as the PCR product from the positive control plasmid. If it runs lower, this implies that the SunTag array was (partially) recombined out from the virus.
30. Clean up the remaining PCR product using PCR or gel cleanup kit, following manufacturer's instructions, and send for sequencing at a commercial vendor to confirm the correct sequence.
    ◆ **TROUBLESHOOTING**
31. Optionally, the virus stock can now be purified and concentrated using sucrose-cushion ultracentrifugation. This is ordinarily not required but might be advisable when the protocol is used to study sensitive processes that might be affected by contaminants that can be contained in the viral stock (for example, cytokines or other host cell proteins). Moreover, it might be useful to concentrate stocks with very low titers. We use a Beckman-Coulter Optima L-90K or Optima XE-90 with a SW32Ti swinging bucket. To do this, prepare 30% sucrose in DPBS and filter sterilize.
32. Put an ultrasensitive scale (digit <0.1 mg) in an appropriate biosafety cabinet along with the rotor insert holders and plastic insert tubes.
33. Add 5 ml of 30% sucrose to the bottom of an appropriate plastic insert tube.
34. Very slowly pipet the virus solution on top of the sucrose cushion, being careful not to disrupt the interface between the virus and sucrose cushion too much. Add up to 28 ml of the virus solution. Add the final amount while placing the plastic insert tube and the corresponding rotor insert holder on a scale and weigh out precisely. Place the plastic insert tube in the metal rotor insert holders with corresponding caps. Place the capped rotor insert holders in the swinging bucket and place the bucket carefully in the ultracentrifuge.
    ▲ **CRITICAL STEP** The tubes should always be at least two thirds full, or they might implode during ultracentrifugation. If this is not possible with virus solution, fill up with DPBS.
    ▲ **CRITICAL STEP** Carefully balance the centrifuge insert. Weight imbalances might cause extremely dangerous situations and damage to the ultracentrifuge.
35. Spin overnight (16 h) at 100,000*g* at 4 °C (this corresponds with 28,000 rpm for our ultracentrifuge and rotor).
    ■ **PAUSE POINT** Samples will run overnight.
36. The next morning, retrieve the rotor insert holders and carefully remove the plastic tubes in an appropriate biosafety cabinet. Carefully aspirate the supernatant and discard until left with the pellet (which usually occurs as a subtle brown-yellow 'stain' on the bottom of the tube).
37. Resuspend the pellet in the desired amount of DPBS (at least 1 ml is advisable) and transfer to tubes. Store at −80 °C.
    ■ **PAUSE POINT** Virus stocks can be stably stored at −80 °C for years.
38. Once a virus stock has been obtained with the correct SunTag insert, the viral titers can be determined using $TCID_{50}$ or plaque assays. We generally use $TCID_{50}$ assays. To do so, first seed the cells of interest (that is, those cells that will be used during the VIRIM assay) at such density to achieve 50–70% confluency the next day in a flat-bottom 96-well plate using 90 µl of medium per well.
39. The next day, add 10 µl of virus stock (or a tenfold dilution thereof to save virus stock; note that if the titer is very low, this might dilute it beyond the detection limit) to each well of the first column of the 96-well plate.
40. Using a multichannel pipette, serially dilute the virus by mixing and transferring 10 µl from column to column, mixing well after each transfer. Leave the last column untreated.
    ▲ **CRITICAL STEP** Certain cells are sensitive to repeated pipetting in the plate (for example, HEK293T). For these cells, it is advisable to do the serial dilution in a separate 96-well plate and transfer the viral dilutions directly onto the cells.
41. Monitor CPE development over time until it is no longer progressing.
42. Using either the Reed–Muench[79] or Spearman–Kärber[77,78] method, calculate the $TCID_{50}$.
    ▲ **CRITICAL STEP** Owing to the different nature of endpoint titration assays and experimental conditions during live cell imaging, slight differences in titers obtained in

both methods might be observed. It is therefore advisable to start the first live-cell imaging experiment with a new viral stock with a range of inoculum dilutions to find the optimal inoculum dilution.

43. Optionally, virus stocks can be passaged to produce a P1 stock (for example, when more virus is required or to assess whether the SunTag array is stably maintained in the viral genome over multiple viral replication cycles or is recombined out). To do so, seed a fresh flask of susceptible cells and infect them at a low MOI (<0.1) with the P0 stock. Process and characterize P1 stocks in a similar fashion as P0 stocks (Steps 20–42).
    ■ **PAUSE POINT** The virus stocks can be stably stored at −80 °C indefinitely.

Stage 3: generation of STAb–GFP reporter cell line

44. Seed HEK293T cells in a six-well plate at a confluency of ~30%.
45. The next day, transfect cells with the lentiviral plasmid (we use the pHR plasmid backbone) encoding STAb–GFP together with the lentiviral helper plasmids psPAX9 and pMD2.G. We typically use the Fugene transfection reagent. First, for each well to be transfected, combine 1.0 µg of STAb–GFP plasmid with 0.4 µg of pMD2.G and 0.6 µg of psPAX2 plasmid in a 1.5-ml tube.
46. Dilute the plasmid mixture in 100 µl of Opti-MEM for each well to be transfected.
47. For each well to be transfected, add 3 µl of Fugene transfection reagent, mix by pipetting and incubate for 10 min at room temperature.
48. Add 100 µl of the transfection mix dropwise to the cells and gently swirl the plate to mix. Incubate at 37 °C overnight.
    ■ **PAUSE POINT** The cells are incubated overnight.
49. A total of 24 h after transfection, use a fluorescence microscope to confirm that at least 25% of the cells are expressing GFP. Remove the medium from the cells and replace with fresh cell culture medium.
    ▲ **CRITICAL STEP** Be very gentle while changing the medium, as HEK293T detach easily from the plate.
50. Three days after transfection collect lentivirus-containing supernatant in a 5 ml Luer-lock disposable syringe. Pass the supernatant through a 0.45-µm filter to remove cellular debris and collect the filtrate in a 15-ml tube.
    ■ **PAUSE POINT** The lentivirus-containing medium can be stored at 4 °C for ~1 week or at −80 °C for several months.
51. Optionally, users can titrate the lentivirus stocks to provide a more precise MOI for subsequent transduction. In our experience, this is not absolutely required if FACS is used later (Step 55) to select low-expressing cells. However, if polyclonal cell populations are directly used instead for VIRIM imaging experiments without prior sorting, this is advisable.
52. Seed the cells that will be transduced in a six-well plate at a confluency of ~30%. In the 'Generation of reporter cell lines' section of the 'Experimental design' section we provide general considerations for the type of cells that can be used for VIRIM.
53. The next day, add ~300 µl of lentivirus-containing medium (from Step 50) to the cells. If the viral stock was titrated, we recommend using an MOI of ~1.
54. Incubate the cells at 37 °C with lentivirus for 2 days for efficient transduction.
    ■ **PAUSE POINT** Cells are incubated for 2 days.
55. Optionally, use FACS to sort individual STAb–GFP expressing cells with optimal expression levels (typically very low) into a 96-well plate filled with 200 µl of conditioned medium per well. If the FACS is not set up in a laboratory of the appropriate biosafety level to work with lentivirus, the cells may need to be cultured for longer, depending on local regulations, to allow their sorting (that is, to ensure no infectious lentivirus remains). To select cells with optimal STAb–GFP expression during FACS sorting, use the nontransduced parental cell line as a negative control to determine baseline autofluorescence signal. Typically, a very low-level expression of STAb–GFP gives an optimal signal-to-noise ratio during a VIRIM experiment, and therefore, the sorting gate is set to exclude high-expressing cells. We typically focus on the lowest ~25% of GFP expressing cells (see Supplementary Fig. 1 for FACS gating strategy). Alternatively, polyclonal cell populations can be used for VIRIM imaging

assays as well, but this is generally suboptimal as divergent STAb–GFP expression levels might affect assay outcomes (for example, VIRIM foci intensities).

56. Expand the single cells into monoclonal cell populations by growing them under optimal growth conditions. Passage them into larger culture vessels when cells reach confluency. Depending on the cell type and its doubling time, this can take anywhere from 2 to 6 weeks. Screen the monoclonal cell lines for homogeneous expression levels of STAb–GFP (that is, cells that do not show GFP foci in the absence of viral infection). Select a clonal cell line with optimal STAb–GFP expression level ('Generation of reporter cell lines' section of the 'Experimental design' section) and freeze aliquots of the cell line.
▲ **CRITICAL STEP** During the initial validation of results, it is advisable to perform VIRIM experiments in multiple monoclonal cell lines to exclude any clone-specific effects.
▲ **CRITICAL STEP** For polyclonal cell lines, it is advisable to test whether expression levels affect assay outcomes (for example, VIRIM spot intensity, phase durations and so on).
■ **PAUSE POINT** Cells can be frozen and stored indefinitely in liquid nitrogen or at −140 °C.

Stage 4: performing a VIRIM imaging experiment

Sample preparation

57. Seed STAb–GFP-expressing reporter cells on a glass-bottom dish that is compatible with time-lapse microscopy. We typically seed cells in a 96-well imaging plate at varying densities and select those wells with a confluency of ~70% at the start of the VIRIM experiment.
▲ **CRITICAL STEP** Be gentle in handling the imaging plate to prevent scratches and ensure that the glass surface remains clean.
■ **PAUSE POINT** Depending on seeding density, cells can typically be maintained in the plate for 1–3 days.
58. Optional: if the experiment involves chemical compounds (for example, inhibitors of host cell factors such as enzymes), pretreatment of the cells before the virus addition may be required. Include the compound in the imaging medium as well, if needed.
59. Before the start of the time-lapse microscopy, dilute the SunTag-CVB3 stock produced in stage 2 in 200 µl of complete Leibovitz's L15 medium, prewarmed to 37 °C at the desired MOI.
▲ **CRITICAL STEP** The use of Leibovitz's L15 medium is required when imaging is performed on a microscope that is not equipped with a CO_2-perfusion chamber. If a CO_2 system is available on the microscope, other types of medium can be used, provided that the medium does not contain compounds that interfere with fluorescence microscopy (for example, phenol red).
▲ **CRITICAL STEP** Depending on the desired read-out of the experiment it is important to choose an appropriate MOI. For most VIRIM experiments, single infections per cell are optimal for downstream analysis. Thus, choose an MOI at which few cells are double-infected while having enough cells with a single infection. For most assays, we find an MOI of 0.25 to be optimal.
60. Replace the normal cell culture medium with 200 µl of SunTag-CVB3-containing Leibovitz's L15 imaging medium and incubate for 30 min at 37 °C.
61. A total of 15 min before imaging, remove the virus-containing medium and replace with Leibovitz's L15 imaging medium (prewarmed to 37 °C).
▲ **CRITICAL STEP** Medium evaporation during time-lapse microscopy could impact cell viability during the experiment. Minimize the evaporation by placing a lid on the imaging dish and add sufficient medium (≥200 µl for a 96-well) at the start of infection. Adding DPBS to the wells directly next to the imaging well also reduces the medium evaporation in the imaging well. Some microscope incubation chambers or plate holders also have reservoirs for water to maintain humidity and prevent excessive evaporation.

Image acquisition

62. Set the temperature control unit of the microscope to 37 °C at least 30 min before the start of infection.
▲ **CRITICAL STEP** The kinetics of virus infection are affected by temperature. Make sure that the temperature at the microscope is stable at 37 °C before imaging.

63. Select an objective that is suitable for the experiment, using the considerations that are provided in the 'Imaging infection' section of the 'Experimental design' section.
64. Add a drop of immersion oil, prewarmed to 37 °C, to the objective and place the imaging plate in the appropriate stage holder. For long-term imaging, it can help to apply some immersion oil to the glass bottom of the imaging plate and spread it using some lens paper.
65. We now provide three general imaging approaches: an imaging scheme that enables long-term visualization of viral infection progression (option A). This scheme can, for example, be used for quantifying the number of translating vRNAs over time. The second imaging scheme (option B) is specifically intended for determining the translation site intensity, and the third scheme (option C) is aimed at quantifying the diffusive properties of single translating vRNAs.

(A) **Long-term VIRIM**

(i) Select multiple *xy*-positions for time-lapse imaging. Several factors determine how many positions can be selected during an experiment, including the imaging interval, exposure time, number of imaging channels and number of *Z*-slices. Select positions where cells have a local confluency of ~90%. Avoid cells that have apparent GFP aggregates or excessive autofluorescence.

(ii) Select the range of *Z*-slices to cover the complete volume of the cells. Use the minimal number of slices required to cover the entire cell. For U2OS cells, this typically requires 10–15 slices at an 0.8-µm interval.

▲ **CRITICAL STEP** Use an automated focusing system to prevent focus drift during time-lapse imaging (for example, NIKON 'perfect focus system' or Olympus '*Z*-drift compensation').

(iii) Specify the imaging duration and acquisition interval. For the quantification of the duration of CVB3 infection phases, we generally image at a 3 min imaging interval for 6 – 8 h. When we combined VIRIM with additional readouts of late-stage infection (that is, occurring after antibody depletion) we generally opt for 5- or 10-min interval to reduce phototoxicity and image for 16–20 h.

(iv) Specify laser power and exposure times. As the translating CVB3 vRNAs are diffusing rapidly through the cytoplasm, the use of long exposure times (>100 ms) may result in motion blur of GFP foci and should be avoided. Use a laser power that is high enough to detect weak viral translation sites but does not result in severe photobleaching (<5% signal decay over 100 frames) or phototoxicity (typically apparent by cell rounding and detachment in uninfected cells).

■ **PAUSE POINT** The cells are imaged overnight.

(B) **Short time-lapse imaging for viral translation site intensity measurements**

(i) Select a single field of view that contains one or more infected cell(s) in which individual translating vRNAs can de be detected. Avoid cells that have apparent GFP aggregates or excessive autofluorescence.

▲ **CRITICAL STEP** If too many translation sites are present in the cell, limiting STAb–GFP availability will result in decreased nascent chain labeling and thereby reduce VIRIM spot intensity. Select cells with a low number of VIRIM foci (<40 foci) to ensure that antibody depletion is not affecting translation site intensities.

(ii) Select the range of *Z*-slices to cover the complete volume of the cells. Use the minimal number of slices required to cover the entire cell. For U2OS cells, this typically requires 10–15 slices at an 0.8 µm interval.

(iii) Specify the number of frames and the acquisition interval. We typically acquire 10 frames at a 50 ms frame rate.

(iv) Use high laser power and a short exposure time (25 ms).

(C) **Short time-lapse imaging for single-molecule tracking**

(i) Select a single field of view that contains one or more infected cell(s) in which individual translating vRNAs can be detected.

▲ **CRITICAL STEP** For successful tracking of individual VIRIM foci it is important that the number of foci in an infected cell is not too high (<20 translating vRNAs).

(ii) Select a single *Z*-slice in the center of the cell.
▲ **CRITICAL STEP** Do not use the automated focus system in this experimental setup, as this may slow down image acquisition, and focus drift is usually negligible during the short time-lapse imaging series.
(iii) Specify the number of frames and the acquisition interval. We typically acquire 100 frames at a 40 ms frame rate.
(iv) Use maximum laser power and a short exposure time (20 ms).
■ **PAUSE POINT** Once imaging has been completed, the protocol can be paused before and during processing and data analysis.

Stage 5: Image processing and data analysis

Imaging data pre-processing

66. Typically, maximum intensity projections are created to reduce image file size and simplify data analysis, if multiple *Z*-slices were acquired (in the NIKON NIS-Elements software select the tab 'Image' > 'ND processing' > 'Create Maximum Intensity Projection Image in Z'). Export the data for further analysis.
▲ **CRITICAL STEP** If data analysis is performed in 3D, or otherwise requires analysis of individual *Z*-slices, no maximum intensity projection should not be made before data export.
67. Flatfield correction (Optional: if VIRIM foci intensity is measured): Non-homogeneous sample illumination and signal detection may result in an apparent signal intensity drop towards the edges of the field of view. For flatfield corrections, an image should be acquired of a slide with homogeneous fluorescence using the same objective (for this we typically use dye solution (for example, 1 µM Atto-488 dye in DPBS) in an imaging plate). This image can then be used to correct uneven illumination in the images. The procedure for performing flatfield correction has been described elsewhere[83].
68. Bleach correction: Repeated laser exposure may result in progressive loss of fluorescent signal because of fluorophore bleaching. To correct for this, determine the average intensity of the entire image for each timepoint, and perform corrections that maintain a constant average image intensity. This correction can be performed using for instance ImageJ (select 'Image' > 'Adjust' > 'Bleach Correction', correction method 'Exponential Fit').

Image analysis

69. We provide three different types of analysis that can be performed on the imaging data: VIRIM infection phase analysis (option A), viral translation site intensity measurements (option B) and single-molecule tracking of translating vRNAs (option C). Each type of analysis is best performed on imaging data that was acquired using the respective image acquisition scheme outlined in Step 64. For the analyses we use the freely available image analysis software ImageJ and various ImageJ plugins.
(A) **VIRIM infection phase analysis**
(i) Open an imaging file in ImageJ that was acquired using the acquisition settings described in Step 65A.
(ii) Determine which cells in the field of view (FOV) are amenable to analysis. Reasons to exclude cells from analysis can include:
- A cell is not completely in the FOV for the entire duration of the analysis
- A cell undergoes mitosis during the analysis period
- At the start of imaging multiple GFP foci are already apparent in the cell, indicating that the virus has already undergone replication or that the cell was infected by multiple viral particles

▲ **CRITICAL STEP** The inclusion and exclusion criteria should be clearly defined beforehand, well documented and applied consistently throughout the analysis to prevent biases in the analysis.
(iii) For each cell that is included in the analysis, determine the number of GFP foci in every timepoint, taking the following aspects into account:
- Because of the high mobility of individual translating vRNAs, the same spot may be detected in multiple *Z*-slices at different *x*,*y* coordinates, resulting in the

appearance of two juxtapositioned foci in the maximum intensity projection. Score two spots that are very close to each other as a single VIRIM spot to prevent overestimating the number of viral translation sites (Fig. 5a, bottom left)

- In some cells, STAb–GFP may accumulate in small aggregates that are present throughout the time-lapse movie. These aggregates are readily discriminated from VIRIM foci as they are less mobile, larger in size and often aberrant in shape (nonspherical). In addition, STAb–GFP may become enriched at centrosomes in several cells, which may result in the appearance of one or two static spots adjacent to the nucleus. Both types of immobile GFP focus should not be scored as VIRIM foci
- STAb depletion will result in decreased labeling efficiency for translating vRNAs and the gradual disappearance of fluorescent foci. For CVB3, this typically means that individual VIRIM foci can no longer be reliably detected when more than 50 foci are present in an infected cell

(iv) Assign infection phases on the basis of the number of VIRIM foci that are observed at each timepoint in the movie. Establish a set of rules to assign infection phases in a consistent manner. See Box 1 for practical details about assigning VIRIM infection phase and Supplementary Table 1 for an exemplary data set.

(v) For every infected cell, determine the duration of each infection phase by multiplying the number of timepoints a cell spends in a phase by the time interval between imaging timepoints.

(vi) We typically present the duration of each infection phase for a cell population as a Kaplan–Meier survival curve, which can be generated using graph generating software (for example, Prism (GraphPad)) or in Excel, using the template provided in Supplementary Table 1. A major advantage of Kaplan–Meier survival curves is that they also include data from aborted infections and infections that could not be tracked over the duration of the entire experiment. To create a Kaplan–Meier survival curve, determine two parameters for each cell: first, whether the infection successfully completed an infection phase (that is, did the cell enter the next phase during the time-lapse movie). Second, determine the time spent in each infection phase. Note that if the infection phase is not completed within the time of recording (for example, because the movie ended or the cell died before the infection phase was finished), the time from the start of the infection phase until the end of the recording or the moment of cell death should still be noted.

(B) **Analysis of viral translation site intensity**

(i) Open an imaging file that was acquired using the acquisition settings described in Step 64B.

▲ **CRITICAL STEP** To perform intensity measurements on VIRIM imaging data, it is important to perform additional postacquisition image corrections (Steps 67 and 68).

(ii) In the preprocessed images, select a cell with viral translation sites and measure the intensity of all VIRIM foci in that cell by positioning an ROI over the center of the translation site and measuring the average intensity in every frame of the time-series (In ImageJ: 'Analyze' > 'Set measurements', select 'Mean gray value' > 'OK'. Position the ROI over the GFP spot 'Analyze' > 'Measure').

▲ **CRITICAL STEP** Use the smallest possible ROI for which all pixels of the focus are located within the ROI. The ROI must have the same dimensions for all measurements. A CVB3 translation site is typically measured using an ROI of 0.6 µm × 0.6 µm.

▲ **CRITICAL STEP** Ensure that all translation sites are measured, not only the brightest ones that are easier to detect. If many translating vRNAs are present in the cell, select a random region of the cell and measure the intensity of all foci in this region of the cell. This will minimize the risk of analysis bias.

(iii) For each translation site, also measure the local background signal in the same manner by randomly positioning the ROI at three locations in the direct proximity of the GFP spot, excluding regions that contain other GFP foci. Measure the local background intensity in each frame of the time series.

(iv) Subtract the average of the three local background intensities from the translation site intensity for each timepoint and determine the average background-subtracted translation site intensity of the time series.

(v) Plot the intensities of multiple viral translation sites in a histogram to visualize the distribution of viral translation site intensities.

(C) **Single-molecule tracking of translating vRNAs (Fig. 6d,e)**

(i) Open an imaging file that was acquired using the acquisition settings described in Step 64C.

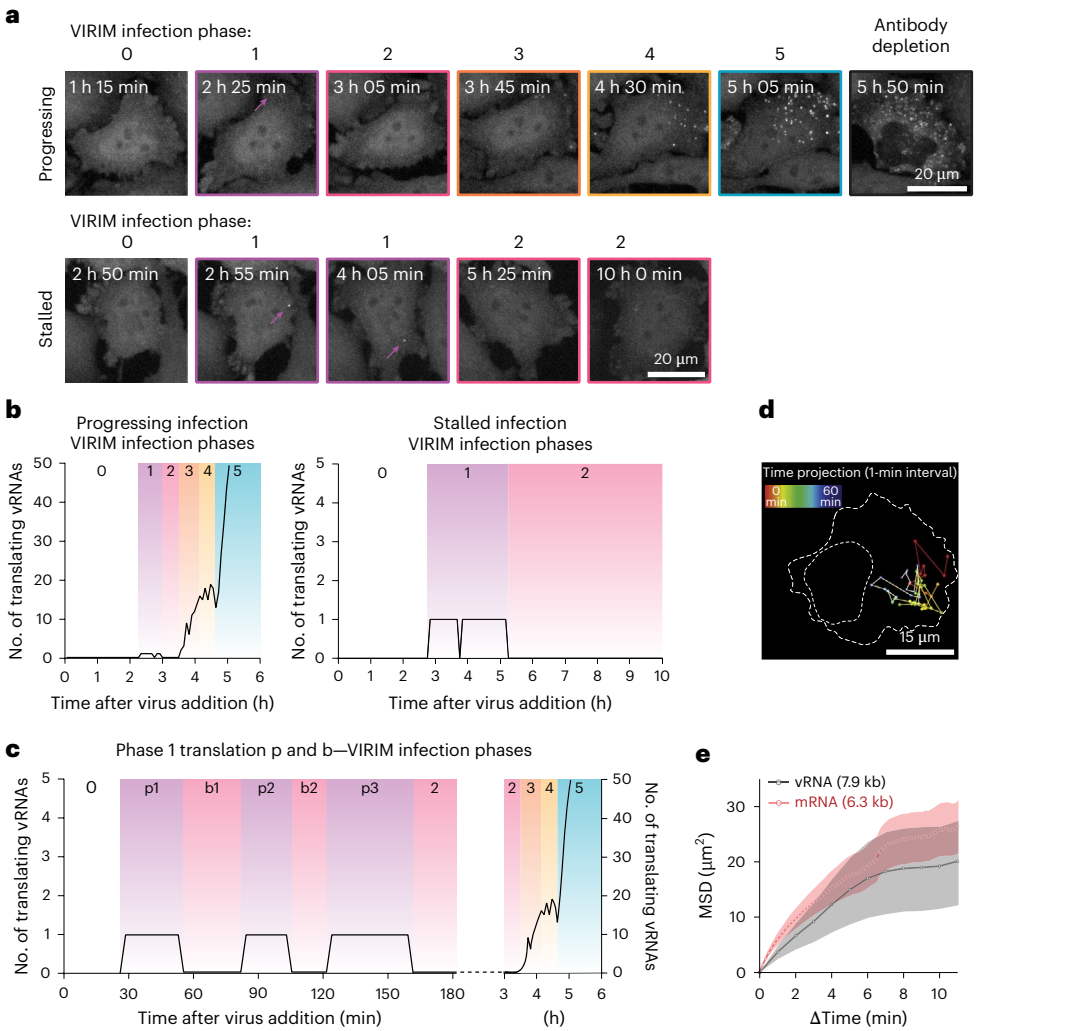

Fig. 6 | VIRIM spot counts, infection phases and single vRNA tracking. a, The images from a movie in which a STAb–GFP-expressing HeLa cell is infected with 5xSunTag-CVB3. Top row: a progressing infection. Bottom row: an infection that is stalled during VIRIM phase 2. The images have colored outlines to highlight the different VIRIM phases (assigned using the VIRIM spot counts shown in **b**). The purple arrows indicate the translation site of the incoming vRNA (VIRIM phase 1 spot). The time is indicated since the moment of virus addition in white text. Scale bars, 20 µm. **b**, The number of translating vRNAs over time since the moment of virus addition for the progressing and the stalled infection that are shown in **a**. VIRIM infection phases were assigned as described in the Protocol and highlighted by the differently colored boxes. **c**, A schematic representation of the translation pulses (p) and replication breaks (b) observed during some infections. The infection presented here eventually undergoes successful replication. The left *y* axis refers covers the curve before the dotted line and the right *y* axis to the curve after the dotted line. **d**, The projection of localization of a single translating vRNA over time. The outlines of the cell and nucleus at the initial timepoint are indicated by dotted lines. The color indicates the time since start initial translation as detected by VIRIM. **e**, This graph depicts a typical mean square displacement (MSD) curve, which gives a measure of the diffusion characteristics of molecules (for example, vRNA molecules being translated). Here, we plotted the relative diffusion speed of translating cellular mRNAs and vRNAs of indicated length. The images in **d** and **e** were adapted with permission from ref. 2, Elsevier.

(ii) Select an infected cell with a limited number of VIRIM foci (<20) (in ImageJ: position an ROI over the cell, run 'Image' > 'Duplicate', select 'Duplicate stack').
(iii) Generate a collection of tracks, composed of the *x*,*y* coordinates of individual translating vRNAs for every time frame. These tracks can be generated by manually annotating spot positions or by using a tracking algorithm (for example, TrackMate). To generate tracks using the TrackMate plugin, firstly select the image time series of the infected cell and open the TrackMate plugin ('Plugins' > 'Tracking' > 'TrackMate'; note that the TrackMate plugin needs to be installed first).
(iv) Select the Laplacian of Gaussian (LoG) detector and adjust the 'estimated blob diameter' and 'Threshold' parameter values such that the VIRIM foci are reliably detected but no other spots are detected in the cell.
(v) Visually inspect whether the automated spot detection performed well. At this stage, TrackMate allows the manual addition and removal of spots that were missed or erroneously detected by the spot calling algorithm. This manual curation is important for optimal performance of the tracking algorithm.
(vi) Select the simple linear assignment problem tracker and adjust the tracking parameters. Set the 'gap-closing max frame gap' to 0 and use small 'linking max distance' (<10 pixels, depending on the pixel size of the microscope camera).
(vii) Visually inspect the track fidelity and exclude or adjust tracks in which VIRIM foci are erroneously linked between timeframes.
(viii) Export spot statistics ('Display options' window > 'Analysis', copy 'Spots in track statistics' window to Excel, compile *x*,*y*-coordinate table for individual tracks).
(ix) Load a table with *x*,*y* tracks in the MATLAB script provided in the Supplementary Software, and calculate the mean square displacements using the instructions provided in the software manual. We typically represent MSD data as in Fig. 6e.

Troubleshooting

Troubleshooting advice can be found in Table 1.

Table 1 | Troubleshooting

Step(s)	Problem	Possible reason	Solution
11	No clear band or a smear is observed on agarose gel when running in vitro transcribed RNA	RNase contamination in any of the preceding steps	Try the entire procedure again with new tips and fresh RNase-free reagents. Optionally, you can add RNase inhibitor to all steps involving RNA
19 and 20	No CPE develops in flasks transfected with either SunTag-virus RNA or in the positive control virus without the SunTag insert	Transfection of infectious RNA failed	Try again with a new preparation of your transfection reagent–RNA complexes. Alternatively, try with another transfection reagent
		Preparation of RNA was not properly purified in Step 10	Redo the purification step using the RNA purification columns
	No CPE develops specifically for the SunTag-virus	Introduction of the SunTag peptide array affects viral fitness	Introduce the SunTag peptide array at a different location in the viral genome
29 and 30	Recovered virus does not contain the SunTag peptide array	The SunTag peptide array was not stably propagated during virus production	Perform a new round of SunTag-virus production and characterization (Steps 13–30). If the array is lost in multiple repeats, introducing the array at a different site in the viral genome may be required
65	It is unclear whether GFP foci represent viral translation sites	STAb–GFP aggregates can be present in the reporter cell	Add the translation inhibitor puromycin (0.1 mg/ml) to cells to confirm that foci are viral translation sites. The GFP foci should completely disappear within ~1 min
			Add a virus replication inhibitor to confirm that the appearance of (additional) GFP foci depends on viral replication
66–69	No GFP foci can be observed	STAb–GFP expression levels are too high	Generate a new reporter cell line with lower STAb–GFP expression levels
		STAb–GFP expression levels are too low	Generate a reporter cell line with higher STAb–GFP expression levels

Table 1 (continued) | Troubleshooting

Step(s)	Problem	Possible reason	Solution
		Viral translation initiation rates are too low; therefore, insufficient numbers of ribosomes are on the vRNA at any given time	Introduce a longer array of SunTag peptides in the viral genome or add an additional sequence downstream of the SunTag array. Both modifications will increase the amount of STAb–GFP associated to each nascent chain and thus increase the signal intensity
		SunTag-virus does not replicate in the STAb–GFP-expressing reporter cell line	Confirm that SunTag-virus is replicating by qPCR. If the viruses indeed fail to replicate, choose a different cell type or position SunTag array at a different location in the viral genome
66–69	VIRIM foci become progressively dimmer (long before antibody depletion)	Photobleaching	Adjust imaging parameters, for example, by lowering the laser power, shortening exposure times and/or increasing frame interval time
66–69	Cells die during time-lapse imaging (both infected and uninfected cells)	Phototoxicity	Adjust imaging parameters, for example, by lowering the laser power, shortening exposure times and/or increasing frame interval time

Timing

Below we give an indication of the time each stage of the Protocol takes.
Stage 1, Step 1, design of SunTag-virus: 1–2 days
Stage 1, Steps 2–5, cloning of plasmids encoding SunTag-virus: 5–10 days
Stage 2, Steps 6–21, producing SunTag-virus: 5–10 days
Stage 2, Steps 22–43, characterizing SunTag-virus: 5–10 days
Stage 3, Steps 44–56, generation of reporter cell line: 21–35 days
Stage 4, Steps 57–65, VIRIM imaging assay: 1–2 days
Stage 5, Steps 66–68, image saving, preprocessing and exporting: 30 min to 2 h
Stage 5, Step 69A, analysis, VIRIM phase analysis: 1–3 days
Stage 5, Step 69B, analysis, viral translation site intensity measurement: 4–8 h
Stage 5, Step 69C, analysis, single-molecule tracking of translating vRNAs: 4–8 h

Anticipated results

If the functional SunTag-virus can be recovered and a good reporter cell line is established, the individual translating viral RNAs can be visualized during infection using this Protocol. Based on the number, intensity and mobility of VIRIM foci, several insights can be gained about viral infection. For reference of what VIRIM imaging of a successful infection looks like, see Supplementary Video 1 and Fig. 5a.

First, the moment of viral entry can be approximated on the basis of the moment of initial appearance of a single GFP spot in reporter cells. Typically, this initial CVB3 translation site can be detected ~30–90 min after the addition of the SunTag-CVB3 virus to reporter cells. Second, the number of infecting viral particles can be determined on the basis of the number of VIRIM foci that appear in the cell during the first 1–2 h. Note that additional infecting viral particles cannot be reliably identified once the replication of the first virus has initiated. Third, after an initial period of CVB3 translation, the CVB3 translation site typically disappears when the vRNA undergoes replication. Successful replication will result in the stepwise increase in the number of translating vRNAs up to the moment antibody depletion, at which point, a decrease in translation site intensity is observed and the assay is completed. By determining the number of VIRIM foci over time, both the dynamics and success rate of viral replication can be determined (Fig. 6a–c). Importantly, for RNA viruses with different viral life cycles, the pattern of VIRIM spot appearance and the moment of antibody depletion may be different. Fourth, in addition to calling viral entry and replication based on the number of VIRIM foci, the mobility of VIRIM foci also reports on important features of the vRNA. Measuring the MSD of vRNAs at different

timepoints during infection or different regions in the cells will reveal whether vRNAs are freely diffusing in the cytoplasm or are tethered to subcellular organelles. For CVB3, freely diffusing vRNAs have an average MSD value[1] of 0.05 $\mu m^2/s$ (note that there is always a broad range of MSD values for individual vRNAs; Fig. 6d,e). The MSD values for freely diffusing vRNAs will depend on the size of the vRNA and the number of proteins associated with the vRNA; therefore, they may differ for other viruses. Finally, the VIRIM spot intensity can be assessed at different timepoints, in different cellular localization or for different viral sequences. The spot intensity reports on the translation efficiency of the vRNA (note that the spot intensity is dependent both on the translation initiation and elongation rates) but also on the moment of nascent chain release, which in turn depends on the design of the SunTag-virus. Relative changes in translation efficiency can be determined by comparing GFP foci intensities under different conditions. Absolute ribosome loads and initiation rates can also be determined, but this requires the precise normalization of the GFP intensity and knowledge of the moment of SunTag nascent chain release from translating ribosomes, and, as such, is challenging in many cases.

Reporting summary

Further information on research design is available in the Nature Portfolio Reporting Summary linked to this article.

Data availability

The source data used to generate the figures are provided via Mendeley Data at https://doi.org/10.17632/v4vnfcycv3.1. This includes two example timelapse imaging files. The additional source data can be retrieved via the primary research article[2].

Code availability

The MATLAB script used for MSD calculations and an instruction for using the script are provided as Supplementary Information, software 1. It can also be accessed via Mendeley Data at https://doi.org/10.17632/v4vnfcycv3.1.

Received: 19 December 2024; Accepted: 2 October 2025;
Published online: 04 December 2025

References

1. Bruurs, L. J. M. et al. Antiviral responses are shaped by heterogeneity in viral replication dynamics. *Nat. Microbiol.* **8**, 2115–2129 (2023).
2. Boersma, S. et al. Translation and replication dynamics of single RNA viruses. *Cell* **183**, 1930–1945.e23 (2020).
3. Jones, J. E., Le Sage, V. & Lakdawala, S. S. Viral and host heterogeneity and their effects on the viral life cycle. *Nat. Rev. Microbiol.* **19**, 272–282 (2021).
4. Heldt, F. S., Kupke, S. Y., Dorl, S., Reichl, U. & Frensing, T. Single-cell analysis and stochastic modelling unveil large cell-to-cell variability in influenza A virus infection. *Nat. Commun.* **6**, 8938 (2015).
5. Zanini, F., Pu, S.-Y., Bekerman, E., Einav, S. & Quake, S. R. Single-cell transcriptional dynamics of flavivirus infection. *eLife* **7**, e32942 (2018).
6. Russell, A. B., Trapnell, C. & Bloom, J. D. Extreme heterogeneity of influenza virus infection in single cells. *eLife* **7**, e32303 (2018).
7. Schulte, M. B. & Andino, R. Single-cell analysis uncovers extensive biological noise in poliovirus replication. *J. Virol.* **88**, 6205–6212 (2014).
8. Guo, F. et al. Single-cell virology: on-chip investigation of viral infection dynamics. *Cell Rep.* **21**, 1692–1704 (2017).
9. Zanini, F. et al. Virus-inclusive single-cell RNA sequencing reveals the molecular signature of progression to severe dengue. *Proc. Natl Acad. Sci. USA* **115**, E12363–E12369 (2018).
10. Russell, A. B., Elshina, E., Kowalsky, J. R., te Velthuis, A. J. W. & Bloom, J. D. Single-cell virus sequencing of influenza infections that trigger innate immunity. *J. Virol.* https://doi.org/10.1128/jvi.00500-19 (2019).
11. Steuerman, Y. et al. Dissection of influenza infection in vivo by single-cell RNA sequencing. *Cell Syst.* **6**, 679–691.e4 (2018).
12. Speranza, E. et al. Single-cell RNA sequencing reveals SARS-CoV-2 infection dynamics in lungs of African green monkeys. *Sci. Transl. Med.* **13**, eabe8146 (2021).
13. Jovic, D. et al. Single-cell RNA sequencing technologies and applications: A brief overview. *Clin. Transl. Med.* **12**, e694 (2022).
14. Dábilla, N. & Dolan, P. T. Structure and dynamics of enterovirus genotype networks. *Sci. Adv.* **10**, eado1693 (2024).
15. Singer, Z. S., Ambrose, P. M., Danino, T. & Rice, C. M. Quantitative measurements of early alphaviral replication dynamics in single cells reveals the basis for superinfection exclusion. *Cell Syst.* **12**, 210–219.e3 (2021).
16. Lee, J. Y. et al. Absolute quantitation of individual SARS-CoV-2 RNA molecules provides a new paradigm for infection dynamics and variant differences. *eLife* **11**, e74153 (2022).
17. Ramanan, V. et al. Viral genome imaging of hepatitis C virus to probe heterogeneous viral infection and responses to antiviral therapies. *Virology* **494**, 236–247 (2016).
18. Schaar, H. M. van der et al. Dissecting the cell entry pathway of dengue virus by single-particle tracking in living cells. *PLoS Pathog.* **4**, e1000244 (2008).
19. Lakadamyali, M., Rust, M. J., Babcock, H. P. & Zhuang, X. Visualizing infection of individual influenza viruses. *Proc. Natl Acad. Sci. USA* **100**, 9280–9285 (2003).
20. Seisenberger, G. et al. Real-time single-molecule imaging of the infection pathway of an adeno-associated virus. *Science* **294**, 1929–1932 (2001).
21. Bächi, T. Direct observation of the budding and fusion of an enveloped virus by video microscopy of viable cells. *J. Cell Biol.* **107**, 1689–1695 (1988).
22. Lowy, R. J., Sarkar, D. P., Chen, Y. & Blumenthal, R. Observation of single influenza virus-cell fusion and measurement by fluorescence video microscopy. *Proc. Natl Acad. Sci. USA* **87**, 1850–1854 (1990).
23. Georgi, A., Mottola-Hartshorn, C., Warner, A., Fields, B. & Chen, L. B. Detection of individual fluorescently labeled reovirions in living cells. *Proc. Natl Acad. Sci. USA* **87**, 6579–6583 (1990).

24. Pelkmans, L., Kartenbeck, J. & Helenius, A. Caveolar endocytosis of simian virus 40 reveals a new two-step vesicular-transport pathway to the ER. *Nat. Cell Biol.* **3**, 473–483 (2001).
25. Suomalainen, M. et al. Microtubule-dependent plus- and minus end–directed motilities are competing processes for nuclear targeting of adenovirus. *J. Cell Biol.* **144**, 657–672 (1999).
26. Coller, K. E. et al. RNA interference and single particle tracking analysis of hepatitis C virus endocytosis. *PLoS Pathog.* **5**, e1000702 (2009).
27. Brandenburg, B. et al. Imaging poliovirus entry in live cells. *PLoS Biol.* **5**, e183 (2007).
28. van der Schaar, H. M. et al. Characterization of the early events in dengue virus cell entry by biochemical assays and single-virus tracking. *J. Virol.* **81**, 12019–12028 (2007).
29. Elliott, G. & O'Hare, P. Live-cell analysis of a green fluorescent protein-tagged herpes simplex virus infection. *J. Virol.* **73**, 4110–4119 (1999).
30. Cruz, S. S. et al. Assembly and movement of a plant virus carrying a green fluorescent protein overcoat. *Proc. Natl Acad. Sci. USA* **93**, 6286–6290 (1996).
31. McDonald, D. et al. Visualization of the intracellular behavior of HIV in living cells. *J. Cell Biol.* **159**, 441–452 (2002).
32. Sun, E.-Z. et al. Real-time dissection of distinct dynamin-dependent endocytic routes of influenza a virus by quantum dot-based single-virus tracking. *ACS Nano* **11**, 4395–4406 (2017).
33. Zhang, L.-J. et al. Lipid-specific labeling of enveloped viruses with quantum dots for single-virus tracking. *mBio* https://doi.org/10.1128/mbio.00135-20 (2020).
34. Liu, H.-Y., Wang, Z.-G., Liu, S.-L. & Pang, D.-W. Single-virus tracking with quantum dots in live cells. *Nat. Protoc.* **18**, 458–489 (2023).
35. Liu, H.-Y. et al. In-situ quantitation of genome release of Japanese encephalitis viruses by quantum dot-based single-virus tracking. *Nano Today* **40**, 101271 (2021).
36. Baggen, J., Thibaut, H. J., Strating, J. R. P. M. & van Kuppeveld, F. J. M. The life cycle of non-polio enteroviruses and how to target it. *Nat. Rev. Microbiol.* **16**, 368–381 (2018).
37. Rand, U. et al. Uncoupling of the dynamics of host–pathogen interaction uncovers new mechanisms of viral interferon antagonism at the single-cell level. *Nucleic Acids Res.* **42**, e109 (2014).
38. Combe, M., Garijo, R., Geller, R., Cuevas, J. M. & Sanjuán, R. Single-cell analysis of RNA virus infection identifies multiple genetically diverse viral genomes within single infectious units. *Cell Host Microbe* **18**, 424–432 (2015).
39. Timm, A. & Yin, J. Kinetics of virus production from single cells. *Virology* **424**, 11–17 (2012).
40. Matula, P. et al. Single-cell-based image analysis of high-throughput cell array screens for quantification of viral infection. *Cytom. Part A* **75A**, 309–318 (2009).
41. Tanenbaum, M. E., Gilbert, L. A., Qi, L. S., Weissman, J. S. & Vale, R. D. A protein-tagging system for signal amplification in gene expression and fluorescence imaging. *Cell* **159**, 635–646 (2014).
42. Wang, C., Han, B., Zhou, R. & Zhuang, X. Real-time imaging of translation on single mRNA transcripts in live cells. *Cell* **165**, 990–1001 (2016).
43. Pichon, X. et al. Visualization of single endogenous polysomes reveals the dynamics of translation in live human cells. *J. Cell Biol.* **214**, 769–781 (2016).
44. Yan, X., Hoek, T. A., Vale, R. D. & Tanenbaum, M. E. Dynamics of translation of single mRNA molecules in vivo. *Cell* **165**, 976–989 (2016).
45. Morisaki, T. et al. Real-time quantification of single RNA translation dynamics in living cells. *Science* **352**, 1425–1429 (2016).
46. Khuperkar, D. et al. Quantification of mRNA translation in live cells using single-molecule imaging. *Nat. Protoc.* **15**, 1371–1398 (2020).
47. Barton, D. J., Morasco, B. J. & Flanegan, J. B. Translating ribosomes inhibit poliovirus negative-strand RNA synthesis. *J. Virol.* **73**, 10104–10112 (1999).
48. Gamarnik, A. V. & Andino, R. Switch from translation to RNA replication in a positive-stranded RNA virus. *Genes Dev.* **12**, 2293–2304 (1998).
49. Hoek, T. A. et al. Single-molecule imaging uncovers rules governing nonsense-mediated mRNA decay. *Mol. Cell* **75**, 324–339.e11 (2019).
50. Mateju, D. et al. Single-molecule imaging reveals translation of mRNAs localized to stress granules. *Cell* **183**, 1801–1812.e13 (2020).
51. Hambidge, S. J. & Sarnow, P. Translational enhancement of the poliovirus 5′ noncoding region mediated by virus-encoded polypeptide 2A. *Proc. Natl Acad. Sci. USA* **89**, 10272–10276 (1992).
52. Kräusslich, H. G., Nicklin, M. J., Toyoda, H., Etchison, D. & Wimmer, E. Poliovirus proteinase 2A induces cleavage of eucaryotic initiation factor 4F polypeptide p220. *J. Virol.* **61**, 2711–2718 (1987).
53. Lamphear, B. J., Kirchweger, R., Skern, T. & Rhoads, R. E. Mapping of functional domains in eukaryotic protein synthesis initiation factor 4G (eIF4G) with picornaviral proteases: implications for cap-dependent and cap-independent translational initiation. *J. Biol. Chem.* **270**, 21975–21983 (1995).
54. Belov, G. A. et al. Early alteration of nucleocytoplasmic traffic induced by some RNA viruses. *Virology* **275**, 244–248 (2000).
55. Flather, D. & Semler, B. L. Picornaviruses and nuclear functions: targeting a cellular compartment distinct from the replication site of a positive-strand RNA virus. *Front. Microbiol.* **6**, 594 (2015).
56. Gustin, K. E. & Sarnow, P. Effects of poliovirus infection on nucleo-cytoplasmic trafficking and nuclear pore complex composition. *EMBO J.* **20**, 240–249 (2001).
57. Park, N., Katikaneni, P., Skern, T. & Gustin, K. E. Differential Targeting of Nuclear Pore Complex Proteins in Poliovirus-Infected Cells. *J. Virol.* **82**, 1647–1655 (2008).
58. Park, N., Schweers, N. J. & Gustin, K. E. Selective removal of FG repeat domains from the nuclear pore complex by enterovirus $2A^{pro}$. *J. Virol.* **89**, 11069–11079 (2015).
59. Schipper, J. G. et al. The multifaceted role of the viral 2A protease in enterovirus replication and antagonism of host antiviral responses. *PLoS Pathog.* **21**, e1013443 (2025).
60. Chen, W., Zhao, X., Yang, N. & Li, X. Single mRNA imaging with fluorogenic RNA aptamers and small-molecule fluorophores. *Angew. Chem. Int. Ed.* **62**, e202209813 (2023).
61. Ouellet, J. RNA fluorescence with light-up aptamers. *Front. Chem.* **4**, 29 (2016).
62. Bühler, B. et al. Avidity-based bright and photostable light-up aptamers for single-molecule mRNA imaging. *Nat. Chem. Biol.* **19**, 478–487 (2023).
63. Beach, D. L., Salmon, E. D. & Bloom, K. Localization and anchoring of mRNA in budding yeast. *Curr. Biol.* **9**, 569–578 (1999).
64. Bertrand, E. et al. Localization of *ASH1* mRNA particles in living yeast. *Mol. Cell* **2**, 437–445 (1998).
65. Tyagi, S. Imaging intracellular RNA distribution and dynamics in living cells. *Nat. Methods* **6**, 331–338 (2009).
66. van der Schaar, H. M. et al. Illuminating the sites of enterovirus replication in living cells by using a split-GFP-tagged viral protein. *mSphere* **1**, e00104–e00116 (2016).
67. Manicassamy, B. et al. Analysis of in vivo dynamics of influenza virus infection in mice using a GFP reporter virus. *Proc. Natl Acad. Sci. USA* **107**, 11531–11536 (2010).
68. Lux, K. et al. Green fluorescent protein-tagged adeno-associated virus particles allow the study of cytosolic and nuclear trafficking. *J. Virol.* **79**, 11776–11787 (2005).
69. Pierson, T. C. et al. An infectious West Nile virus that expresses a GFP reporter gene. *Virology* **334**, 28–40 (2005).
70. Kittel, C. et al. Rescue of influenza virus expressing GFP from the NS1 reading frame. *Virology* **324**, 67–73 (2004).
71. Das Sarma, J., Scheen, E., Seo, S., Koval, M. & Weiss, S. R. Enhanced green fluorescent protein expression may be used to monitor murine coronavirus spread in vitro and in the mouse central nervous system. *J. Neurovirol.* **8**, 381–391 (2002).
72. Domínguez, J., Lorenzo, M. M. & Blasco, R. Green fluorescent protein expressed by a recombinant vaccinia virus permits early detection of infected cells by flow cytometry. *J. Immunol. Methods* **220**, 115–121 (1998).
73. Klump, W. M., Bergmann, I., Müller, B. C., Ameis, D. & Kandolf, R. Complete nucleotide sequence of infectious Coxsackievirus B3 cDNA: two initial 5′ uridine residues are regained during plus-strand RNA synthesis. *J. Virol.* **64**, 1573–1583 (1990).
74. Wessels, E., Duijsings, D., Notebaart, R. A., Melchers, W. J. G. & van Kuppeveld, F. J. M. A proline-rich region in the coxsackievirus 3A protein is required for the protein to inhibit endoplasmic reticulum-to-Golgi transport. *J. Virol.* **79**, 5163–5173 (2005).
75. Otsuki, K., Maeda, J., Yamamoto, H. & Tsubokura, M. Studies on avian infectious bronchitis virus (IBV). *Arch. Virol.* **60**, 249–255 (1979).
76. Desmyter, J., Melnick, J. L. & Rawls, W. E. Defectiveness of interferon production and of rubella virus interference in a line of African green monkey kidney cells (Vero). *J. Virol.* **2**, 955–961 (1968).
77. Spearman, C. The method of right and wrong cases (constant stimuli) without Gauss's formulae. *Br. J. Psychol.* **2**, 227–242 (1908).
78. Kärber, G. Beitrag zur kollektiven Behandlung pharmakologischer Reihenversuche. *Arch. Exp. Path. Pharm.* **162**, 480–483 (1931).
79. Reed, L. J. & Muench, H. A simple method of estimating fifty per cent endpoints. *Am. J. Epidemiol.* **27**, 493–497 (1938).
80. Dulbecco, R. Production of plaques in monolayer tissue cultures by single particles of an animal virus. *Proc. Natl Acad. Sci. USA* **38**, 747–752 (1952).
81. Lambert, G. G. et al. Aequorea's secrets revealed: new fluorescent proteins with unique properties for bioimaging and biosensing. *PLoS Biol.* **18**, e3000936 (2020).
82. Tinevez, J.-Y. et al. TrackMate: an open and extensible platform for single-particle tracking. *Methods* **115**, 80–90 (2017).
83. Model, M. Intensity calibration and flat-field correction for fluorescence microscopes. *Curr. Protoc. Cytom.* **68**, 10.14.1–10.14.10 (2014).

Acknowledgements

We thank H. Rabouw for providing the FACS data that is presented in Supplementary Fig. 1 and for helpful discussions during the review process. We thank S. Boersma, who was critical in the initial development of the VIRIM technology. We thank S. Yang for providing the MATLAB script and instructions for calculating the MSD. We thank the members of the Tanenbaum lab and van Kuppeveld lab for helpful discussions. This work was financially supported by an NWO klein-2 grant (grant no. OCENW.KLEIN.344) to M.E.T. and F.J.M.v.K and by EU Horizon 2024 ERC Advanced Grant project VIRLUMINOUS (grant no. 01053576) to F.J.M.v.K. L.J.M.B. and M.E.T. were supported by the Oncode Institute, which is partly funded by the Dutch Cancer Society (KWF).

Author contributions

L.J.M.B. and J.G.S. made the figures. L.J.M.B., J.G.S., F.J.M.v.K. and M.E.T. wrote the manuscript.

Competing interests

The authors declare no competing interests.

Additional information

Supplementary information The online version contains supplementary material available at https://doi.org/10.1038/s41596-025-01290-1.

Correspondence and requests for materials should be addressed to Frank J. M. van Kuppeveld or Marvin E. Tanenbaum.

Peer review information *Nature Protocols* thanks Urs Greber and the other, anonymous, reviewer(s) for their contribution to the peer review of this work.

nature portfolio

Corresponding author(s): Marvin E. Tanenbaum
Frank J.M. van Kuppeveld

Last updated by author(s): Aug 16, 2025

Reporting Summary

Nature Portfolio wishes to improve the reproducibility of the work that we publish. This form provides structure for consistency and transparency in reporting. For further information on Nature Portfolio policies, see our Editorial Policies and the Editorial Policy Checklist.

Statistics

For all statistical analyses, confirm that the following items are present in the figure legend, table legend, main text, or Methods section.

n/a	Confirmed
☒	☐ The exact sample size (*n*) for each experimental group/condition, given as a discrete number and unit of measurement
☒	☐ A statement on whether measurements were taken from distinct samples or whether the same sample was measured repeatedly
☒	☐ The statistical test(s) used AND whether they are one- or two-sided *Only common tests should be described solely by name; describe more complex techniques in the Methods section.*
☒	☐ A description of all covariates tested
☒	☐ A description of any assumptions or corrections, such as tests of normality and adjustment for multiple comparisons
☒	☐ A full description of the statistical parameters including central tendency (e.g. means) or other basic estimates (e.g. regression coefficient) AND variation (e.g. standard deviation) or associated estimates of uncertainty (e.g. confidence intervals)
☒	☐ For null hypothesis testing, the test statistic (e.g. *F*, *t*, *r*) with confidence intervals, effect sizes, degrees of freedom and *P* value noted *Give P values as exact values whenever suitable.*
☒	☐ For Bayesian analysis, information on the choice of priors and Markov chain Monte Carlo settings
☒	☐ For hierarchical and complex designs, identification of the appropriate level for tests and full reporting of outcomes
☒	☐ Estimates of effect sizes (e.g. Cohen's *d*, Pearson's *r*), indicating how they were calculated

Our web collection on statistics for biologists contains articles on many of the points above.

Software and code

Policy information about availability of computer code

Data collection	We used a custom-made MATLAB script, which is available as as supplementary software package, which also includes instructions on how to use it. We used both NIS Elements software from Nikon and CellSens from Olympus Evident to operate the microscopes.
Data analysis	We made use of ImageJ for basic image processing. For data processing and visualization we used Microsoft Excel and Graphpad PRISM software.

For manuscripts utilizing custom algorithms or software that are central to the research but not yet described in published literature, software must be made available to editors and reviewers. We strongly encourage code deposition in a community repository (e.g. GitHub). See the Nature Portfolio guidelines for submitting code & software for further information.

Data

Policy information about availability of data

All manuscripts must include a data availability statement. This statement should provide the following information, where applicable:

- Accession codes, unique identifiers, or web links for publicly available datasets
- A description of any restrictions on data availability
- For clinical datasets or third party data, please ensure that the statement adheres to our policy

Source data used to generate the figures are provided via Mendeley Data: 10.17632/v4vnfcycv3.1. This includes two example timelapse imaging files. Additional

source data can be retrieved via the primary research article.

Research involving human participants, their data, or biological material

Policy information about studies with human participants or human data. See also policy information about sex, gender (identity/presentation), and sexual orientation and race, ethnicity and racism.

Reporting on sex and gender	NA
Reporting on race, ethnicity, or other socially relevant groupings	NA
Population characteristics	NA
Recruitment	NA
Ethics oversight	NA

Note that full information on the approval of the study protocol must also be provided in the manuscript.

Field-specific reporting

Please select the one below that is the best fit for your research. If you are not sure, read the appropriate sections before making your selection.

☒ Life sciences ☐ Behavioural & social sciences ☐ Ecological, evolutionary & environmental sciences

For a reference copy of the document with all sections, see nature.com/documents/nr-reporting-summary-flat.pdf

Life sciences study design

All studies must disclose on these points even when the disclosure is negative.

Sample size	NA
Data exclusions	NA
Replication	NA
Randomization	NA
Blinding	NA

Reporting for specific materials, systems and methods

We require information from authors about some types of materials, experimental systems and methods used in many studies. Here, indicate whether each material, system or method listed is relevant to your study. If you are not sure if a list item applies to your research, read the appropriate section before selecting a response.

Materials & experimental systems

n/a	Involved in the study
☒	☐ Antibodies
☐	☒ Eukaryotic cell lines
☒	☐ Palaeontology and archaeology
☒	☐ Animals and other organisms
☒	☐ Clinical data
☒	☐ Dual use research of concern
☒	☐ Plants

Methods

n/a	Involved in the study
☒	☐ ChIP-seq
☐	☒ Flow cytometry
☒	☐ MRI-based neuroimaging

Eukaryotic cell lines

Policy information about cell lines and Sex and Gender in Research

Cell line source(s)	HEK293T cells (ATCC, cat. no. CRL-3216, RRID: CVCL_0063) U2OS cells (ATCC, cat. no. HTB-96, RRID: CVCL_0042) BHK-21 C13 (ATCC, cat. no. CCL-10, RRID: CVCL_1915) Vero-E6 (ATCC, cat. no. CRL-1586, RRID: CVCL_0574)

	HeLa cells (RRID: CVCLM763)
Authentication	cells were not authenticated.
Mycoplasma contamination	cell lines were regularly tested for mycoplasm and found to be negative.
Commonly misidentified lines (See ICLAC register)	HeLa cells.

Plants

Seed stocks	NA
Novel plant genotypes	NA
Authentication	NA

Flow Cytometry

Plots

Confirm that:

☒ The axis labels state the marker and fluorochrome used (e.g. CD4-FITC).

☒ The axis scales are clearly visible. Include numbers along axes only for bottom left plot of group (a 'group' is an analysis of identical markers).

☒ All plots are contour plots with outliers or pseudocolor plots.

☒ A numerical value for number of cells or percentage (with statistics) is provided.

Methodology

Sample preparation	*Describe the sample preparation, detailing the biological source of the cells and any tissue processing steps used.*
Instrument	Beckman-Coulter CytoFLEX SRT.
Software	CytExpert; FLOWJO
Cell population abundance	Ungated: 6134 Live cells: 2780 Single cells: 2378 GFP+ total: 580 GFP+ Q1: 238
Gating strategy	First the population of live cells is selected based on FSC-A/SSC-A profile. Next, single cells are distinguished from doublets based on FSC-A vs FSC-H profiles, which correlate linearly for single cells but not doublets/clumps. Finally, based on a non-transduced control cell sample the GFP-positive population (in the 525-40(488) parameter) is selected and within this population cells are sorted from the lowest 25% expressing cells.

☒ Tick this box to confirm that a figure exemplifying the gating strategy is provided in the Supplementary Information.